

# VP-Bench: A Comprehensive Benchmark for Visual Prompting in Multimodal Large Language Models

Mingjie Xu<sup>1\*</sup>, Jinpeng Chen<sup>2\*</sup>, Yuzhi Zhao<sup>2†</sup>, Jason Chun Lok Li<sup>3</sup>, Yue Qiu<sup>4</sup>, Zekang Du<sup>4</sup>, Mengyang Wu<sup>5</sup>, Pingping Zhang<sup>2</sup>, Kun Li<sup>2</sup>, Hongzheng Yang<sup>5</sup>, Wenao Ma<sup>5</sup>, Jiaheng Wei<sup>1</sup>, Qinbin Li<sup>4</sup>, Kangcheng Liu<sup>6</sup>, Wenqiang Lei<sup>7</sup>

<sup>1</sup>The Hong Kong University of Science and Technology (Guangzhou)

<sup>2</sup>City University of Hong Kong

<sup>3</sup>The University of Hong Kong

<sup>4</sup>Huazhong University of Science and Technology

<sup>5</sup>The Chinese University of Hong Kong

<sup>6</sup>Hunan University

<sup>7</sup>Sichuan University

mingjiexu@hkust-gz.edu.cn, jinpeng.chen@my.cityu.edu.hk, yzzhao2-c@my.cityu.edu.hk

## Abstract

Multimodal Large Language Models (MLLM) have enabled a wide range of advanced vision-language applications, including fine-grained object recognition and contextual understanding. When querying specific regions or objects in an image, human users naturally use “Visual Prompts” (VP) like bounding boxes to provide reference. However, no existing benchmark systematically evaluates the ability of MLLMs to interpret such VPs. This gap raises uncertainty about whether current MLLMs can effectively recognize VPs, an intuitive prompting method for humans, and utilize them to solve problems. To address this limitation, we introduce VP-Bench, aiming to assess MLLMs’ capability in VP perception and utilization. VP-Bench employs a two-stage evaluation framework: Stage 1 examines models’ ability to perceive VPs in natural scenes, utilizing 30K visualized prompts spanning 8 shapes and 355 attribute combinations. Stage 2 investigates the impact of VPs on downstream tasks, measuring their effectiveness in real-world problem-solving scenarios. Using VP-Bench, we evaluate 28 MLLMs, including proprietary systems (e.g., GPT-4o) and open-source models (e.g., InternVL3 and Qwen2.5-VL). In addition, we provide a comprehensive analysis of factors affecting VP understanding, such as variations in VP attributes, question arrangement, and model scale. VP-Bench establishes a new reference framework for studying MLLMs’ ability to comprehend and resolve grounded referring questions.

Datasets — <https://github.com/Endlinc/VP-Bench>

## Introduction

The emergence of multimodal large language models (MLLM) (OpenAI 2023, 2024; Liu et al. 2023) has spurred research into their applications across diverse downstream

tasks. For example, a user can verbally instruct the model to recognize furniture in indoor 3D scenes (Zhou et al. 2024b; Zhang et al. 2024c; Zhou et al. 2024a), ground wild animals in their natural environment as depicted in an image (Rasheed et al. 2024; Zhang et al. 2024a), use external knowledge to determine a piece of furniture’s brand and price, and provide insights into the habits of those wild animals. Beyond object detection via natural-language queries, researchers have explored MLLMs’ ability to interpret user-drawn annotations (e.g., freehand regions) and identify interactions involving target instances in context (Cai et al. 2024; Fu et al. 2024). Consequently, visual prompts (VP), graphical cues such as bounding boxes and alphabet tags, have emerged to direct model attention, offering an intuitive alternative to verbal descriptions. However, MLLMs still underperform human annotators in grounded referring tasks with VPs. To quantify this gap, ViP-Bench (Cai et al. 2024) was introduced, comprising 303 image-question pairs across eight VP types in practical scenarios (e.g., OCR, mathematical reasoning). Although ViP-Bench provides valuable insights into region reasoning, it does not assess, first, how perceptible different VP styles are to models. For example, while bounding boxes are ubiquitous, their low-contrast or overly thin edges may be difficult for models to detect, limiting task accuracy. Moreover, it remains unclear whether adding distinctive corner markers to a bounding box VP would further enhance performance. Second, how variations in VP design affect downstream performance. For example, consider a lung region that is suspected to contain a malignant lesion. Is the application of an additional overlaying VP on this area more effective in directing the model’s attention compared to specifying the region’s location within the verbal instruction, while still maintaining the contextual information?

To address these questions, we conduct a comprehensive review of prior studies (Cai et al. 2024; Fu et al. 2024; Zhang et al. 2024a; Rasheed et al. 2024; Yang et al. 2023) to catego-

\*These authors contributed equally.

†Corresponding Author.

Copyright © 2026, Association for the Advancement of Artificial Intelligence ([www.aaai.org](http://www.aaai.org)). All rights reserved.

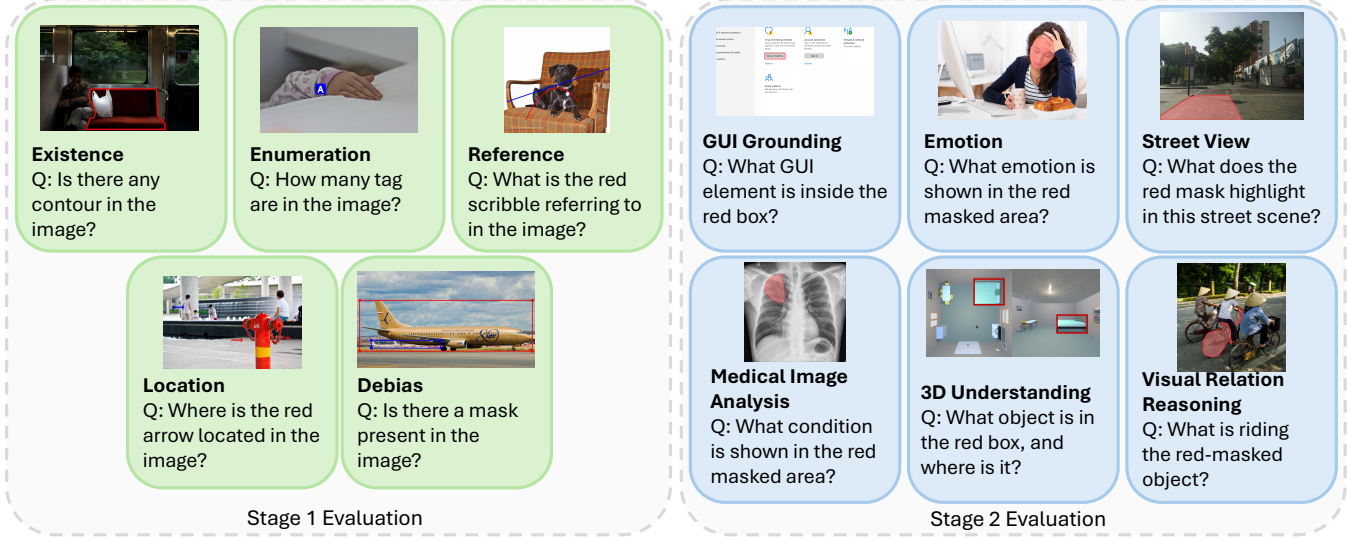


Figure 1: Overview of the VP-Bench Dataset. VP-Bench introduces a two-stage evaluation framework: (1) **Model Perception**, which assesses general VP recognition capabilities using 30K visualized VPs spanning five question types; and (2) **VP Effect on Downstream Tasks**, which evaluates the impact of visual prompts on various downstream applications. All questions follow a multiple-choice format, but the full list of options is not displayed due to space limitations.

Benchmark	# Images	# VP	Domains	Debias
SoV	119	$\approx 5$	1	No
ViP-Bench	303	8	1	No
VP-Bench	<b>34 267</b>	<b>355</b>	4	Yes

Table 1: Comparison of three VP-related benchmarks. We list the number of images, number of VP attribute combinations, the image domains covered, and whether each dataset includes debias questions.

riize commonly employed VP shapes and their corresponding variants, which we subsequently define as attributes. We classify VP shapes into eight categories: tag, bounding box, arrow, mask, contour, oval, point, and scribble. Each category shares general attributes such as line width and color, and may also incorporate shape-specific attributes, including style or content format. A detailed overview of the VP shapes and their associated attributes is provided in the supplementary materials. In total, our proposed VP-Bench encompasses 355 unique VP attribute permutations. The benchmark consists of more than 30,000 distinct image–question pairs, constructed to evaluate core VP capabilities, including existence, enumeration, referencing, and spatial localization. This component constitutes Stage 1 of VP-Bench. Furthermore, to examine the influence of VP on downstream task performance, we introduce six tasks that incorporate VP reasoning as a second stage, thereby reflecting the model’s ability to leverage VP reasoning in real-world problem-solving contexts. Additional examples from the benchmark are provided in Figure 1, and a concise comparison between VP-Bench and other VP-related benchmarks is presented in Table 1.

We evaluate a range of popular MLLMs on our VP-Bench, including proprietary systems (e.g., GPT-4o) and open-source models (e.g., InternVL3 and Qwen2.5-VL). In Stage 1, we analyze the influence of factors such as instruction arrangement, model parameters, VP shapes, and attributes on model performance. In Stage 2, we examine the models’ capabilities across various VP-enabled downstream tasks, evaluating their ability to integrate visual cues with textual context, distinguish fine-grained object features, and leverage domain-specific knowledge. Moreover, we complement quantitative metrics with qualitative analyses to highlight each model’s interpretability and reliability in real-world scenarios. This comprehensive evaluation not only benchmarks current capabilities but also identifies potential areas for improvement, thereby informing future research in multimodal interaction and model interpretability.

To summarize, our contributions are as follows:

- We introduce VP-Bench, a two-stage evaluation framework for assessing MLLMs. Stage 1 measures VP perception capability in natural scenes, while Stage 2 evaluates the ability to integrate VP understanding for practical problem-solving. Compared to existing benchmarks, our evaluation is significantly more comprehensive and includes over 100 times as many images.
- In stage 1, we examine the effects of 355 attribute combinations across eight VP shapes, covering a scale more than 40 times larger than previous studies. In Stage 2, we assess six VP-enabled downstream tasks, offering a comprehensive reference for real-world applications.
- Our results highlight the critical role of VP shape in model performance. Regular shapes (e.g., bounding boxes, ovals) are generally more efficient than irregular ones (e.g., masks, contours), even though the latter pro-

vide finer spatial details. Including VP shape descriptions in prompts further improves contextual understanding. Selecting VP shapes suited to the application scenario is more impactful than relying on the model’s preferred shape in a general scenario.

## Related Works

### Multimodal Large Language Models

Building on the recent success of neural language processing, particularly through LLM approaches, researchers have increasingly integrated visual understanding and reasoning to expand these models’ capabilities (Chen et al. 2022; Huang et al. 2023; OpenAI 2023; Li et al. 2023; Liu et al. 2023). Several studies have introduced visual instruction tuning (Liu et al. 2023) and specialized architectures (Li et al. 2023) for MLLMs, leading to significant advancements in image comprehension and common-sense reasoning. However, many existing MLLMs lack dedicated models or data designs for referring expressions or location-based referencing. Consequently, some researchers have adopted mask encoders to focus attention on specific regions (Guo et al. 2024), while others craft targeted text prompts to highlight region (Wang et al. 2024b). For instance, RegionGPT (Guo et al. 2024) and LLaVA-Grounding (Zhang et al. 2024a) employ additional mask encoders to improve location comprehension, though this adds computational overhead and demands retraining when introducing newer base models or additional VP shapes. Alternatively, approaches such as SoM (Yang et al. 2023), ViP-LLaVA (Cai et al. 2024), and ControlMLLM (Wu et al. 2024) demonstrate that sketching VPs directly on images can substantially enhance various downstream region-referring tasks. Yet, evaluations of these models’ handling of visually marked images have largely been qualitative, and comprehensive quantitative assessments across diverse region-referring tasks remain limited.

### MLLM Benchmarks

Benchmarking MLLMs is crucial for exposing model limitations and guiding future development (Yue et al. 2024; Yu et al. 2024; Meng et al. 2025; Ying et al. 2024; Liu et al. 2024; Guan et al. 2024). Although many existing benchmarks assess perception and reasoning, they largely emphasize image-level tasks. A few incorporate referring expression questions (Wei et al. 2024; Zhang et al. 2024a; Li et al. 2025), yet often neglect the role of VPs in visual understanding. For instance, RefCOCO (Kazemzadeh et al. 2014) evaluates referring expression capabilities but lacks VP-oriented image design, while HC-RefLoCo (Wei et al. 2024) extends expression length without addressing the contribution of VPs to regional comprehension in MLLMs. Recently, researchers have worked on developing VP-oriented benchmarks, such as the SoV (Zhang et al. 2024b) validation dataset and ViP-Bench (Cai et al. 2024), to provide a more thorough evaluation of VP cognition. However, these benchmarks still fall short when it comes to assessing the impact of VP on MLLM awareness and its effect on downstream

Key Statistics	
Statistic	Number
Total samples	38,932
Total images	34,267
VP Properties	
Shapes	8
Attributes	78
Colors	5
Debias Question	
Without Visualized VP	4.5%
Incorrect Model VP Instruction	8%

Table 2: Key statistics for the dataset. This table provides an overview of the total number of samples, images, and tasks, as well as the debias question amount over the total benchmark.

tasks. For instance, while ViP-Bench offers a relatively comprehensive evaluation of VPs, it does not fully address the variations in VP shapes, attributes, and their effectiveness. These factors are crucial to understanding how different VPs influence MLLMs’ visual comprehension and their potential to improve downstream task performance.

In contrast, our VP-Bench combines a broader range of VP shapes, attributes, and colors with a thorough examination of how VPs affect MLLM performance on various tasks. This comprehensive approach enables a more detailed assessment of model capabilities, providing insights into how VPs can be optimized for better task outcomes.

## VP-Bench

### Overview

VP-Bench is designed to assess the perception of VPs by MLLMs and to evaluate the impact of VPs on downstream task performance. Specifically, VP-Bench comprises 34,267 images and 38,932 multiple-choice questions. In constructing VP-Bench, we meticulously categorized VP shapes and attributes and developed a two-stage evaluation protocol. The Stage 1 data curation process assesses VP perception, while the Stage 2 data curation process examines the influence of VPs on models’ regional perception in downstream tasks.

Compared to existing VP-related benchmarks, VP-Bench introduces several key improvements (see Table 1). First, by incorporating a substantially larger set of test samples, VP-Bench covers an extensive range of VP attribute combinations and diverse grounded referring expression tasks. In Stage 1, it evaluates MLLMs’ perception across all 355 VP attribute combinations, exceeding the scope of other benchmarks by more than 40 times. This diversity compels models to develop a deeper understanding of visual information across various VP types. Second, in Stage 2, we determine the optimal VP combinations for each model and employ them to evaluate six downstream tasks within grounded referring scenarios, a critical gap that previous VP-focused

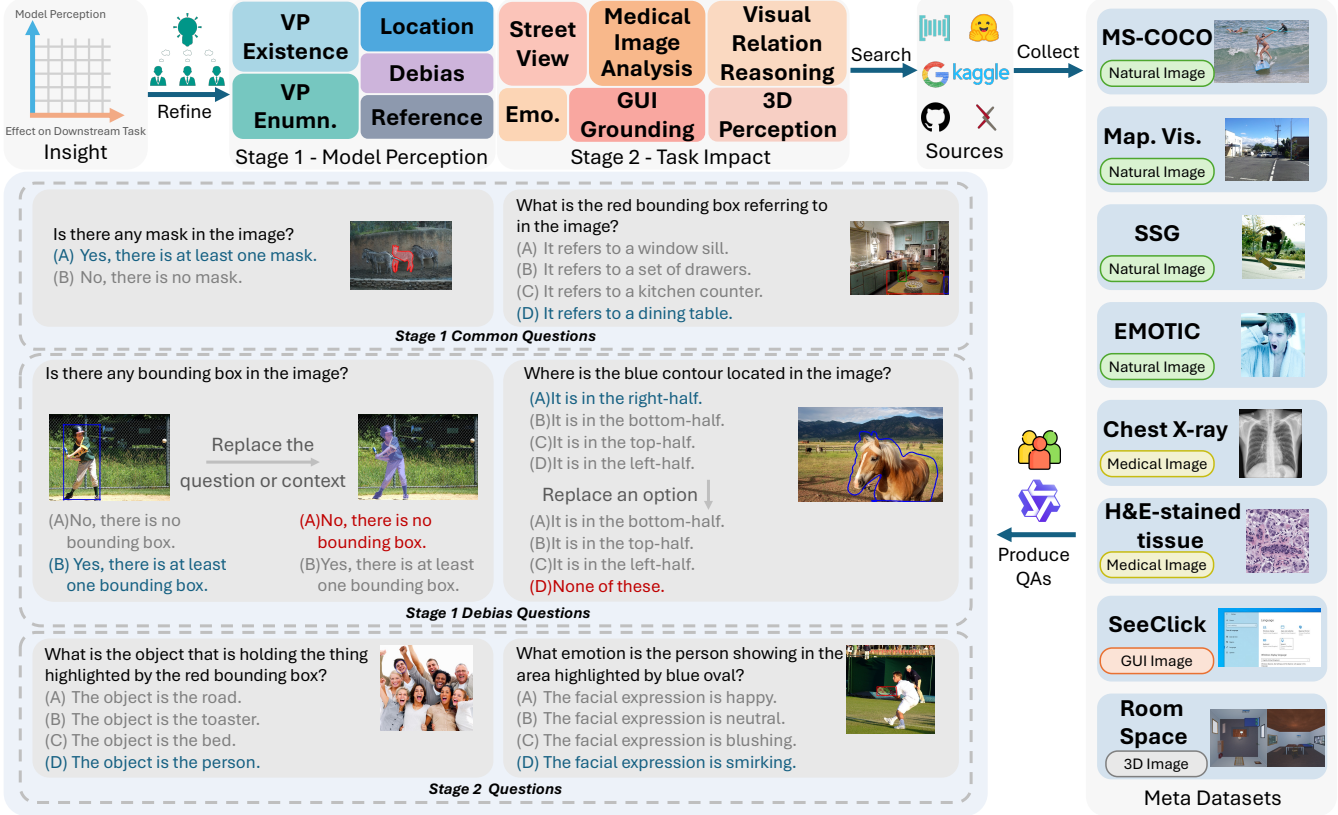


Figure 2: An illustration of our pipeline for data collection. Stage 1 is used to determine the general capabilities of MLLMs in recognizing VPs, while Stage 2 clarifies the impact of using VPs on downstream tasks.

frameworks have yet to fully address. Additionally, we introduce debias questions, where either the images lack the VP type mentioned in the question or all substantively descriptive answer choices are incorrect (see Figure 2) to mitigate unreliable conclusions arising from MLLMs’ hallucinations regarding VP presence. Detailed statistics of VP-Bench are provided in Table 2.

Leveraging the rich data available in VP-Bench, our analytical framework enables a comprehensive evaluation of both VP perception and VP-based referring tasks. The top-down hierarchical structure of VP attributes allows for comparative analyses of models’ perception capabilities across various attributes. Moreover, the diverse downstream referring expression tasks facilitate performance estimation in practical scenarios, helping to delineate in-domain from out-of-domain tasks. Finally, the evaluation samples can be used to assess task learning difficulty, offering valuable insights for optimizing model training and dataset design. A detailed data curation breakdown is provided in the complementary material.

## Visual Prompt Description

The VP description is designed to explicitly verbalize the spatial cues conveyed by visual prompts, rather than relying on the model to infer their meaning solely from the im-

age. As summarized in Table 8, each VP shape encodes a distinct type of spatial signal (e.g., region extent, outline). However, without a corresponding textual description, these cues remain implicit and may be underutilized by current MLLMs. To address this gap, we propose a unified VP description scheme that converts each visual prompt into a short, structured phrase appended to the instruction. For example, a Bounding Box is described as “the red box outlining the target region”. This mapping makes the semantics of each VP shape explicit in language. This design offers two key benefits. First, it reduces ambiguity by explicitly stating whether a mark denotes a point or region. Second, it improves vision–language alignment by mirroring the same spatial cue in both the image and the text, guiding the model to the correct region. Empirically, we observe consistent gains from adding VP descriptions, especially for complex shapes, showing that explicit textual VP semantics are key to fully leveraging visual prompts in MLLMs.

## Stage 1 Data Curation Process

VPs play a pivotal role in guiding model attention and addressing complex problems. In Stage 1 evaluation, we treat VPs as visual cues defined by their intrinsic shapes, attributes, and colors, enabling more targeted information retrieval. We design the VP attributes according to a top-down

VP Shape	Context
Tag	A tag is a small label located at the center of a target, displaying a number or letter. It may be in red, blue, green, or black, and can be circular or square in shape.
Bounding Box	A bounding box is a rectangular frame that marks a target, which may be in red, blue, green, or black.
Arrow	An arrow is a symbol that points to a target, which may be in red, blue, green, or black.
Mask	A mask is a filled area used to indicate a target region, which may be in red, blue, green, or black.
Contour	A contour is the outline of a target, which may be in red, blue, green, or black. It can be drawn precisely along the outline or may resemble a loosely hand-drawn line.
Oval	An oval is an elliptical shape that encircles a target, which may be in red, blue, green, or black.
Point	A point is a square or circular dot that represents a target, located at the center of the marked target, which may be in red, blue, green, or black.
Scribble	A scribble is a random hand-drawn line that indicates a target, which may be in red, blue, green, or black.

Table 3: Definitions of the eight visual prompt (VP) shapes used in our benchmark. Each shape provides a distinct spatial cue (e.g., location, extent, or outline of the target) that is embedded into the model instructions.

hierarchical structure. Initially, we categorize VPs by shape, such as tag, bounding box, arrow, mask, contour, oval, point, and scribble, and further subdivide them by finer-grained attributes and colors. The specific VP shapes and their corresponding attributes are listed in the supplementary materials. The data in Stage 1 primarily comes from the MS-COCO dataset (Lin et al. 2014) due to its segmentation and bounding box annotations. These annotations are essential for generating VPs and their associated question-answer pairs to assess the capabilities of MLLMs.

To define the properties of each VP shape, we begin with a detailed breakdown. A **tag** has attributes including: (1) an alphabet or digit label at its center, with a circular or square shape, and (2) font size specifying the label’s dimensions. A **bounding box** is defined by: (1) line width, representing the thickness of its outline, and (2) vertex shape, such as small squares or circles at the corners. An **arrow**, pointing from a selected direction to the target, has: (1) line width, and (2) pointer shape, which could be triangular or wedge-shaped. A **mask** is a filled region indicating the target, possibly accompanied by an outline, and consists of: (1) line width, and (2) style, which could either be a filled region with or without an outline. A **contour** captures the target’s outline, characterized by: (1) line width, and (2) style, which may be

precise or hand-drawn. An **oval** is an elliptical shape encircling the target, defined by the line width. A **point** is a small square or circular dot located at the target’s center, described by: (1) point size (the area it occupies), and (2) point shape (square or circle). Finally, a **scribble** is a free-form line used to indicate a target, defined by the line width of the scribble.

To evaluate the effect of VPs on visual perception, fine-grained multiple-choice questions were generated for each VP type, covering presence, location, enumeration, and referring objects, with up to four answer options depending on the question type. First, question templates were created manually with guidance from GPT-4o (OpenAI 2024), and annotated answers from metadata were inserted into these templates. Second, distractors were produced either through manually crafted rules or by employing Qwen2-VL-72B (Wang et al. 2024a) with carefully designed prompts to ensure plausibility and quality. For instance, in “reference” questions, Qwen2-VL-72B generated realistic but incorrect options, whereas for “VP spatial location” questions, distractors were sampled based on randomized canvas positions. To enhance evaluation robustness, one debiased sample was included for every six entries. A debiased question consists of a visual image that excludes the VP referenced in the question, together with its corresponding QA pair, as illustrated by the *debias* example in the Stage 1 evaluation in Figure 1.

Overall, the Stage 1 data curation process establishes a comprehensive foundation for evaluating MLLMs’ VP perception capabilities in a controlled setting. By systematically defining VP shapes, attributes, and associated QA pairs, this stage isolates the model’s ability to interpret visual cues independent of downstream reasoning tasks. The resulting dataset enables fine-grained benchmarking of core VP competencies and serves as the basis for the Stage 2 evaluation, where VP understanding is integrated into complex, task-oriented scenarios.

## Stage 2 Data Curation Process

Stage 1 evaluates the performance of different VP types and models in natural scenes. Following this, a new question arises: Can VPs contribute to a broader range of VP-related downstream tasks? How well do existing models perform in this regard? Hence, in Stage 2 evaluation, we carefully select several widely used application scenarios, such as natural recognition, medical image analysis, human facial recognition, street view recognition, traffic sign recognition, visual relation reasoning, GUI recognition, and 3D understanding, which are further categorized into 6 tasks. To investigate whether VPs enhance MLLMs’ regional perception under downstream task scenarios, we evaluate both open-source MLLMs and proprietary systems, using each model’s best-performing VP from Stage 1 results.

For data curation, the target scenarios were first defined, followed by the specification of downstream tasks for each scenario. Relevant datasets were collected through searches on Google, Papers with Code, and Kaggle, and each dataset’s suitability and relevance were systematically evaluated. The data were then organized into a standardized metadata format that includes task descriptions, questions,

answers, input contexts, regional annotations, and images. This standardized format facilitated the construction of visual question–answer pairs, and the accuracy of the information was manually verified to ensure its compatibility with multiple-choice question generation. To maintain efficiency, each task was limited to a maximum of 200 randomly selected images with relevant entries, unless the dataset contained fewer samples. A detailed description of the metadata format is provided in the supplementary materials. The final collection comprises datasets including SZ-CXR (Stirenko et al. 2018), Gleason2019 (Nir et al. 2018), SD-100 (Li, Hogg, and Cohn 2024), Emotic (Kosti et al. 2020), MapillaryVistas (Neuhold et al. 2017), SeeClick (Cheng et al. 2024), and PSG (Yang et al. 2022). These were grouped into six downstream tasks: Medical Image Analysis (MIA) using SZ-CXR and Gleason2019; 3D object recognition using SD-100; facial emotion recognition using Emotic; street view recognition using MapillaryVistas; GUI element recognition using SeeClick; and scene graph generation (SGG) using PSG.

For question and answer generation, we adapt multiple-choice visual questions (with up to four options), drawing from each sample’s metadata. We either craft rules manually or use Qwen2-VL-72B (Wang et al. 2024a) with carefully designed prompts to ensure efficient and high-quality generation. For instance, in 3D question-answering tasks, Qwen2-VL-72B generates plausible but incorrect distractors based on the question and the correct answer, while in visual relation reasoning tasks, we randomly select misleading item classes from the metadata as alternative options.

In summary, the Stage 2 dataset extends the evaluation of VPs beyond controlled natural scenes to diverse, task-driven scenarios. By leveraging the best-performing VP configurations from Stage 1, this stage enables a systematic assessment of how visual prompting contributes to regional perception and task-specific reasoning across multiple application domains. The curated datasets and standardized question–answer pairs provide a robust foundation for benchmarking MLLMs in realistic downstream contexts, thereby bridging the gap between VP perception and practical deployment.

## Experiment

### Experiment Setup

**Compared Models.** In this study, we selected 3 proprietary models along with 24 open-source MLLMs across various categories. These include popular visual models (e.g., Qwen2.5-VL, InternVL-3, and Llama-3.2-Vision), specialized models (e.g., MiniCPM-V 2.6, CogVLM2, and GLM-4V), and recently introduced vision-language architectures (e.g., NVLM, DeepSeek-VL2, Ovis2, and Molmo). To further illustrate the impact of model parameter scale and architecture on visual understanding, we incorporated models of different scales from the InternVL3 and Qwen2.5-VL families.

**Evaluation Metrics.** Our proposed VP-Bench is comprised of two stages, both stages are in multi-choice question format, e.g., “Where is VP located? Options: (A)

In the bottom, (B) In the top”. Generally, we follow the VLMEvalKit (Duan et al. 2024) procedure to evaluate models’ performance. Accuracy is the primary metric.

### Evaluation Main Results

This section evaluates MLLMs on VP-Bench alongside Human baselines. We report the overall score for all perceptual tasks in Table 13 as well as the best performance on each downstream task in Table 5. Various instruction arrangements for all tasks are investigated. We summarize the key findings as follows.

In Stage 1 evaluation, we present the average accuracy of all models across eight VP shapes and four question types in Table 13, along with the human baseline. “Avg.” denotes the average accuracy across all QA samples. In terms of overall accuracy, InternVL3-78, InternVL3-38B, and Molmo-72B rank among the top three, with accuracy around 87%. Other statistics are as follows.

Across all **question types**, most models accurately detect, count, and localize VP, achieving over 90% accuracy on existence queries, around 85% on enumeration queries, and over 92% on rough-location queries. Their performance on referring-expression resolution remains substantially lower: mean accuracy hovers around 70%, and the community favored Qwen-2.5-VL-72B reaches only 75.79%. When benchmarked against human annotators, MLLMs still exhibit an around 10% deficit.

An appropriate **VP shape** can significantly enhance a model’s ability to detect both the prompt and the highlighted region. For example, the bounding box shape is generally a better comparison to the point shape in Table 13, as models can achieve an average of 87.49% with the bounding box shape, but only 67.22% accuracy with the point shape. As well as reflecting most of the models’ best recognized **VP attributes** combination, there are variations of the bounding box shape in Table 5. The results indicate that a contrast color bounding box with medium thickness is optimal for more than half of the models, while a contrast color oval with thin edges is also the most effective for many models, where the contrast color is selected as one of the most distinctive red, green, or blue hues relative to the background. Overall contrast color emerges as the preferred choice for most models. This suggests that color plays a crucial role in distinguishing the region of interest from the background. Regarding scale, thin to medium scale VP yields better results, implying that MLLMs exhibit greater perceptual sensitivity to thin prompts while preserving more contextual information.

### Results Analysis

To further interrogate our preliminary findings, we carried out a series of supplementary experiments whose results yielded several salient statistical patterns. These additional tests not only corroborate the baseline trends but also uncover nuanced insights into the models’ behavior under varying prompt conditions. The remainder of this section highlights the principal observations before delving into a detailed, case-by-case analysis.

Model	Visual Prompt Types								Problem Types				Avg.
	Tag	Arrow	BBox	Contour	Mask	Oval	Point	Scribble	Enumeration	Existence	Rough-Loc.	VP-Ref.	
<i>Human Baseline</i>													
Human Reviewers	89.00	92.62	97.29	87.68	85.28	94.87	90.68	82.80	90.73	94.36	97.68	84.26	90.03
<i>Proprietary Models</i>													
GPT-4o	69.95	70.27	74.18	77.18	65.32	79.77	49.28	64.45	60.44	87.03	57.83	67.74	68.80
Doubaoo-Seed-1.6	86.21	79.60	93.60	72.43	71.19	50.17	47.49	62.30	62.47	64.04	95.34	<b>80.53</b>	70.37
Qwen-VL-Max	92.27	82.84	93.10	88.75	67.51	92.84	69.31	74.45	81.80	88.11	92.13	76.82	82.63
<i>Pre-trained Models</i>													
LLaVA-1.5-7B	67.41	66.75	69.29	64.25	67.35	67.72	59.45	49.36	62.92	96.69	45.54	53.28	63.95
CogVLM2-LLama3-Chat-19B	74.54	69.96	79.56	75.01	48.22	81.54	40.75	43.47	71.87	57.97	73.26	64.13	64.88
InternVL3-1B	74.99	79.91	78.59	75.51	56.00	84.06	58.68	63.93	79.56	67.49	78.83	63.45	71.46
Qwen2.5-VL-3B-Instruct	87.16	79.91	85.41	80.18	52.18	84.58	55.76	64.10	73.07	76.89	89.20	65.29	73.41
LLaVA-1.5-13B	77.98	73.48	77.80	78.47	75.90	76.78	73.17	68.82	83.17	<b>98.77</b>	60.17	60.58	75.47
Llama-3.2-90B-Vision-Instruct	69.17	79.71	91.49	88.71	74.28	91.69	59.28	71.79	77.89	81.51	79.23	71.76	78.45
DeepSeek-VL2	87.36	78.07	80.62	82.24	72.44	75.76	76.80	66.20	73.92	91.41	80.86	71.37	77.94
LLaVA-OneVision-Qwen2-7B-OV	89.36	81.67	88.09	88.89	66.97	92.89	60.76	69.99	79.80	84.99	91.47	69.43	79.58
InternVL3-2B	89.17	84.73	88.92	87.46	57.15	87.79	79.08	69.87	81.41	88.12	89.70	70.23	82.27
GLM-4V-9B	85.43	79.62	87.17	86.65	74.00	85.84	75.46	74.71	<b>91.37</b>	91.44	70.77	74.20	82.36
Qwen2.5-VL-7B-Instruct	90.39	82.94	91.19	88.25	66.51	91.51	67.41	73.08	83.47	86.81	92.10	70.17	81.29
Qwen2.5-VL-32B-Instruct	91.11	82.97	92.04	87.41	69.29	93.64	75.29	74.13	83.94	90.13	91.31	73.49	83.22
InternVL3-14B	91.14	85.17	93.03	90.42	70.47	94.67	73.83	69.64	83.18	89.73	93.51	74.75	83.54
Qwen2.5-VL-72B-Instruct	92.26	82.57	92.88	88.62	68.68	92.83	69.58	74.77	81.84	88.26	92.01	75.79	82.80
Ovis2-34B	91.86	84.39	93.03	90.63	69.49	94.38	72.09	72.49	84.72	88.19	92.49	75.59	83.24
InternVL3-8B	91.25	84.94	92.86	<b>92.83</b>	71.60	93.52	70.52	75.35	86.68	89.13	94.19	72.50	84.11
LLaVA-v1.6-34B-HF	90.89	86.00	86.46	86.59	77.61	91.11	<b>84.28</b>	76.86	82.62	94.97	93.86	72.24	84.97
InternVL3-9B	92.19	<u>86.81</u>	93.76	90.68	73.01	94.21	70.61	78.73	86.51	88.12	93.41	77.37	85.00
NVLM-D-72B	91.28	<b>88.23</b>	91.60	90.22	76.02	93.35	77.00	75.41	83.82	93.99	92.06	76.50	85.39
Molmo-72B-0924	90.71	85.31	92.92	89.61	79.05	93.18	76.57	77.56	87.18	<u>97.24</u>	92.46	70.08	85.61
InternVL3-38B	92.73	86.49	<b>94.33</b>	92.28	77.15	93.86	78.88	<u>79.37</u>	87.84	91.61	<b>95.37</b>	77.93	<u>86.89</u>
InternVL3-78B	<b>93.87</b>	85.77	<u>94.25</u>	91.56	80.01	<b>95.81</b>	<u>81.59</u>	<b>80.89</b>	<u>88.59</u>	92.93	95.24	<u>79.65</u>	<b>87.97</b>
<i>Fine-tuned with Visual-Prompt Data</i>													
ViPLLaVA-13B	75.00	53.02	84.37	86.27	<b>83.79</b>	56.31	46.66	59.50	80.36	61.43	87.70	57.28	68.12
ViPLLaVA-7B	76.44	69.78	81.71	83.78	75.47	65.77	65.38	62.30	77.51	84.84	83.01	53.58	72.58
<b>Average</b>	85.26	79.66	87.49	85.00	69.88	85.02	67.22	69.39	79.92	85.62	84.03	70.21	78.61

Table 4: Performance on VP-shape and question-type subtasks, sorted by overall accuracy. Best of each task excluding human baseline is **bold** and second-best is underlined.

**Shape regular VPs are more readily perceived by MLLMs than shape irregular ones.** As shown in Table 13, models recognize regular VPs like Tag, Arrow, Bounding Box, Oval, at around 80% accuracy on average, whereas for irregular VPs like Mask, Point, Scribble, they only reach less than 70%. Moreover, the gap relative to the human baseline is larger on those irregular shapes. A per-model breakdown shows that InternVL3-78B, while still 9.79% behind humans on Point, differs by only about 2% on Mask and Scribble, and even exceeds human performance on irregular contours (91.56% compared to 87.68%). Notably, DeepSeek-VL2 and InternVL3-14B suffer their worst scores on hand-drawn scribbles. This pattern suggests that training data are biased toward regular geometric forms, with fewer examples of irregular shapes, which in turn impairs MLLMs' ability to detect those VP forms.

**An explicit description of VP shapes is critical for enabling MLLMs to interpret them in context.** To examine whether models truly understand VPs, we compared two settings: with and without a VP-shape description inserted into the instruction. As shown in Table 6, experiments were conducted on InternVL3-78B and Qwen2.5-VL-72B, incorporating VP descriptions consistently enhanced the models' comprehension of VPs, though the effect varied across VP types. For instance, when VP descriptions were included in the **Arrow** and **Contour** scenarios, InternVL3-78B achieved only marginal improvements of 0.32% and 1.37%, respectively, while Qwen2.5-VL-72B improved by just 0.61% and 0.81%. In contrast, substantial gains were observed in the

**Mask** and **Point** scenarios: InternVL3-78B improved by 29.24% and 12.38%, respectively, whereas Qwen2.5-VL-72B improved by 27.3% in the **Mask** scenario but declined by 3.05% in the **Point** scenario. These differences are likely influenced by the distribution of training data, where the frequency of each VP type affects the extent to which descriptive prompts enhance model performance. Collectively, these results suggest that providing an explanatory language description of the VP can help models more accurately identify and interpret the corresponding visual cue in the image.

**VPs that a model perceives most accurately are generally the best choices for downstream tasks but not always.** To investigate this, we devised two selection schemes:

1. **Random Best VP (R-BVP):** is randomly selected from the set of VP attribute combinations that achieved the highest perception performance across all models in the Stage 1 evaluation.
2. **Best VP (BVP):** always uses the single VP attribute combination the current model perceives most accurately.

As shown in Table 5, for Qwen-2.5-VL-72B, the performance gap between BVP and R-BVP stays within  $\pm 5\%$ , and in over half of the tasks BVP outperforms R-BVP. Likewise, InternVL3-78B shows slightly better results with BVP in five tasks, for example, a +5.85% gain on MIA and +1.00% on SD-100, and only trails by 0.26% on SeeClick. By contrast, DeepSeek-VL2 exhibits much larger disparities: in most downstream evaluations, BVP underperforms R-BVP (-11.71% on MapillaryVistas and -19.43% on SeeClick), yet it exceeds R-BVP by +1.68% on MIA. A

Model	Best Attribution Combination	MIA		SD-100		Emotic		Mapillary Vistas		SeeClick		SGG		Average	
		R-BVP	BVP (Δ)	R-BVP	BVP (Δ)	R-BVP	BVP (Δ)	R-BVP	BVP (Δ)	R-BVP	BVP (Δ)	R-BVP	BVP (Δ)	R-BVP	BVP (Δ)
<i>Proprietary Models</i>															
Douba-Seed-1.6	bbox(contrast, round, thick)	<b>57.56</b>	59.60 (+2.04)	<b>87.00</b>	<b>89.33</b> (+2.33)	<b>72.95</b>	70.48 (-2.47)	<b>78.54</b>	76.08 (-2.46)	<b>98.01</b>	97.22 (-0.79)	<b>95.91</b>	<b>96.18</b> (+0.27)	81.66	81.48 (-0.18)
GPT-4o	Tag(digit, blue, round, small)	<b>54.72</b>	60.60 (+6.35)	74.00	72.24 (-1.76)	65.61	66.04 (+0.43)	68.78	57.89 (-10.89)	97.44	97.00 (-0.44)	81.79	81.60 (-0.19)	73.64	72.56 (-1.08)
Qwen-VL-Max	bbox(contrast, none, medium)	42.83	44.32 (+1.49)	80.67	81.27 (+0.60)	74.02	73.03 (-0.99)	64.39	62.68 (-1.71)	96.30	96.89 (+0.59)	<b>95.37</b>	95.44 (+0.07)	75.60	75.61 (+0.01)
<i>Pre-trained Models</i>															
CogVLM2-LLama3-Chat-19B	oval(contrast, thin)	4.20	5.40 (+1.20)	27.67	31.33 (+3.66)	<b>74.40</b>	70.71 (-3.69)	29.27	33.49 (+4.22)	70.17	<b>75.31</b> (+5.14)	<b>84.36</b>	83.30 (-1.06)	48.35	49.92 (+1.57)
DeepSack-VL2	tag(alphabet, green, round, large)	19.22	20.90 (+1.68)	24.75	23.00 (-1.75)	66.18	63.76 (-2.42)	36.59	24.88 (-11.71)	86.93	67.50 (-19.43)	88.20	83.30 (-1.90)	53.15	47.22 (-5.93)
GLM-4V-9B	contour(contrast, contour, thick)	19.12	18.19 (-0.93)	61.00	59.33 (-1.67)	66.67	64.94 (-1.73)	43.90	53.59 (+9.69)	96.59	96.25 (-0.34)	88.62	86.32 (-2.30)	62.65	63.10 (+0.45)
InternVL3-1B	oval(contrast, thin)	19.72	17.20 (-2.52)	47.00	46.67 (-0.33)	57.25	47.14 (-10.11)	40.98	43.54 (+2.56)	91.48	92.90 (+1.42)	88.89	88.45 (-0.44)	57.55	55.98 (-1.57)
InternVL3-2B	bbox(contrast, none, thick)	38.64	40.40 (+1.76)	46.67	51.33 (+4.66)	66.18	<b>66.67</b> (+0.49)	47.32	54.07 (+6.75)	94.60	98.46 (+3.86)	89.96	90.23 (+0.27)	63.89	66.86 (+2.97)
InternVL3-3B	bbox(blue, round, medium)	45.55	46.60 (+1.05)	65.67	75.00 (+9.33)	<b>74.64</b>	71.76 (-2.88)	49.76	52.63 (+2.87)	97.73	97.50 (-0.23)	92.62	93.87 (+1.25)	71.00	72.89 (+1.89)
InternVL3-9B	bbox(contrast, square, thin)	47.75	48.90 (+1.15)	69.33	76.33 (+7.00)	73.43	<b>74.29</b> (+0.86)	56.59	61.72 (+5.13)	96.31	98.15 (+1.84)	90.93	91.83 (+0.90)	72.39	72.89 (+2.81)
InternVL3-14B	bbox(contrast, square, thin)	30.83	29.90 (-0.93)	71.33	77.33 (+6.00)	<b>74.40</b>	72.86 (-1.54)	<b>58.54</b>	61.72 (+3.18)	97.16	98.77 (+1.61)	92.62	93.07 (+0.45)	70.81	72.27 (+1.46)
InternVL3-38B	bbox(red, square, thick)	46.65	48.40 (+1.75)	<b>85.00</b>	88.67 (+3.67)	71.98	72.94 (+0.96)	59.02	59.81 (+0.79)	98.58	99.00 (+0.42)	93.24	94.23 (+0.99)	75.74	77.17 (+1.43)
InternVL3-78B	bbox(red, none, medium)	47.55	<b>53.40</b> (+5.85)	<b>86.00</b>	87.00 (+1.00)	72.95	73.65 (+0.70)	<b>65.37</b>	67.46 (+2.09)	98.01	97.75 (-0.26)	<b>94.67</b>	95.03 (+0.36)	<b>77.42</b>	<b>79.05</b> (+1.63)
Llama-3.2-90B-Vision-Instr.	bbox(green, square, medium)	54.75	59.50 (+4.75)	60.00	58.00 (-2.00)	61.59	65.65 (+4.06)	46.83	51.20 (+4.37)	97.44	98.50 (+1.06)	86.13	88.99 (+2.86)	67.79	70.31 (+2.52)
LLaVA-1.5-7B	tag(digit, red, square, medium)	29.53	35.30 (+5.77)	29.67	31.00 (+1.33)	41.06	33.65 (-7.41)	11.71	13.88 (+2.17)	82.39	83.50 (+1.11)	83.47	73.87 (-9.60)	46.31	45.20 (-1.11)
LLaVA-1.5-13B	tag(alphabet, red, square, large)	37.94	30.60 (-7.34)	27.67	24.00 (-3.67)	49.52	39.76 (-9.76)	19.51	17.22 (-2.29)	84.66	80.25 (-4.41)	87.02	83.30 (-3.72)	51.05	45.85 (-5.20)
LLaVA-OneVision-Qwen-7B-OV-HF	oval(blue, thick)	18.02	16.72 (-1.30)	60.33	63.67 (+3.34)	65.13	64.39 (-0.74)	41.46	47.37 (+5.91)	97.16	98.50 (+1.34)	91.56	92.01 (+0.45)	62.28	63.78 (+1.5)
LLaVA-V1.6-34B-HF	oval(contrast, thin)	39.84	37.60 (-2.24)	48.00	52.33 (+4.33)	68.12	64.05 (-4.07)	42.93	48.33 (+5.40)	94.03	96.30 (+2.27)	92.09	91.30 (-0.79)	64.17	64.98 (+0.81)
MiniCPM-V2.6	tag(digit, red, square, large)	14.61	15.30 (+0.69)	55.00	38.00 (-17.00)	72.22	67.06 (-5.16)	40.49	26.32 (-14.17)	96.02	92.75 (-3.27)	89.96	89.08 (-0.88)	61.38	54.75 (-6.63)
Molmo-72B-0924	bbox(contrast, square, thin)	<b>61.46</b>	<b>62.80</b> (+1.34)	78.00	78.00 (+0.00)	67.63	67.38 (-0.25)	63.41	60.77 (-2.64)	95.17	96.30 (+1.13)	90.93	91.83 (+0.90)	<b>76.10</b>	<b>76.18</b> (+0.08)
NVLM-D-72B	bbox(red, square, thick)	53.45	58.10 (+4.65)	71.33	77.00 (+5.67)	69.08	72.71 (+3.63)	51.22	49.76 (-1.46)	94.60	97.00 (+2.40)	93.69	93.43 (-0.26)	72.23	74.67 (2.44)
Ovis-2-34B	bbox(contrast, square, thin)	33.93	37.30 (+3.37)	78.33	83.33 (+5.00)	74.40	73.10 (-1.30)	53.66	50.72 (-2.94)	<b>99.15</b>	<b>99.69</b> (+0.54)	<b>93.69</b>	<b>94.58</b> (+0.89)	72.19	73.12 (+0.93)
Qwen2.5-VL-3B-Instr.	bbox(red, none, medium)	22.92	23.80 (+0.88)	68.67	66.00 (-2.67)	68.84	68.24 (-0.60)	39.02	44.02 (+5.00)	95.74	98.00 (+2.26)	94.49	94.49 (+0.00)	64.95	65.76 (+0.81)
Qwen2.5-VL-7B-Instr.	bbox(contrast, square, medium)	22.12	22.50 (+0.38)	76.00	77.33 (+1.33)	69.32	70.71 (+1.39)	43.90	52.63 (+8.73)	96.59	<b>99.07</b> (+0.22)	92.62	92.27 (-0.35)	66.76	69.08 (+2.32)
Qwen2.5-VL-72B-Instr.	bbox(contrast, none, medium)	32.00	39.60 (+7.60)	75.33	80.00 (+4.67)	65.71	66.43 (+0.72)	53.85	47.37 (-6.48)	<b>97.73</b>	97.84 (+0.11)	93.24	94.32 (+1.08)	69.64	70.93 (+1.29)
Qwen2.5-VL-72B-Instr.	bbox(contrast, square, thin)	42.44	43.80 (+1.36)	81.67	83.33 (+1.66)	73.91	71.43 (-2.48)	64.88	61.72 (-3.16)	96.59	97.53 (+0.94)	<b>95.20</b>	<b>95.47</b> (+0.27)	<b>75.78</b>	<b>75.55</b> (-0.23)
<b>Average</b>		35.75	37.39 (+1.64)	60.81	61.96 (+1.15)	66.55	64.96 (-1.59)	47.32	47.35 (0.02)	93.34	93.23 (-0.11)	90.46	90.01 (-0.45)		

Table 5: Performance comparison on VP-related tasks. “Best VP Attr. Comb.” indicates the Stage 1 attribute combination. Best in each task is **bold** and second-best is underlined.

Model	Tag	Arrow	BBox	Contour	Mask	Oval	Point	Scribble	Avg.
<i>InternVL3-78B</i>									
w/o VP description	91.69	<b>85.45</b>	94.06	90.19	50.77	92.49	69.21	76.52	81.30
w. VP description	93.87	<b>85.77</b>	94.25	91.56	80.01	<b>95.81</b>	81.59	80.89	87.97
<i>Qwen2.5-VL-72B-Instruct</i>									
w/o VP description	85.93	81.96	92.88	87.81	41.38	82.80	72.63	69.76	76.89
w. VP description	92.26	82.57	92.88	88.62	68.68	92.83	69.58	74.77	82.77

similar pattern appears with GPT-4o: BVP is +6.35% better on MIA but -10.89% worse on MapillaryVistas. These findings suggest that, although a model’s perception accuracy is generally the main criterion for choosing a VP, a robust VP-selection strategy is also critical for maximizing downstream performance.

**Simply training models with VP data offers no clear benefit.** ViP-LLaVA extends the LLaVA architecture by incorporating VP-related data during the instruction tuning stage to enhance VP perception, while LLaVA-1.5 serves as the baseline model in our experiments for comparison against ViP-LLaVA trained with VP-enriched datasets. In Stage 1, LLaVA-1.5-7B achieved an average accuracy of 64.33%, whereas ViP-LLaVA-7B reached 73.01%. However, in Stage 2 downstream tasks, ViP-LLaVA-7B underperformed LLaVA-1.5-7B by 2.88% on MapillaryVistas and by 3.25% on SeeClick. Furthermore, this straightforward training approach led to degradation at larger scales: ViP-LLaVA-13B’s Stage 1 accuracy dropped by 4.13% relative to ViP-LLaVA-7B and by 6.72% relative to LLaVA-1.5-13B. These findings indicate that downstream performance depends more on a model’s robust foundational capabilities and that improving VP perception without compromising these core abilities requires more balanced data composition and refined training strategies.

## Conclusion

We introduce VP-Bench, a two-stage evaluation framework for assessing the capabilities of MLLMs in perceiving VP and solving grounded referring queries. In Stage 1, we construct a dataset of over 30,000 VP images, covering 8 distinct VP shapes and 355 attribute combinations, to evaluate a model’s general understanding of VPs. Our results show that while MLLMs perform well in VP recognition and object counting, they struggle with spatial localization and fine-grained understanding. Additionally, existing models exhibit a preference for bounding boxes and tags and show heightened sensitivity to red VPs. In Stage 2, we introduce 6 VP-related downstream tasks to evaluate how well models integrate VP perception for practical problem-solving. Experimental results suggest that VPs offer certain advantages over text-based spatial prompts for these tasks. However, model performance remains largely dependent on domain knowledge. Overall, this work aims to highlight the need to refine VP attribute representations and enhance spatial reasoning, ultimately improving model interpretability and real-world applicability.

## Acknowledgments

This work is supported by the National Natural Science Foundation of China (Grant No. 62502174).

## References

Cai, M.; Liu, H.; Mustikovela, S. K.; Meyer, G. P.; Chai, Y.; Park, D.; and Lee, Y. J. 2024. ViP-LLaVA: Making large multimodal models understand arbitrary visual prompts. In *Proceedings of the IEEE/CVF Conference on Computer Vision and Pattern Recognition*, 12914–12923.

Chen, J.; Guo, H.; Yi, K.; Li, B.; and Elhoseiny, M. 2022. Visualgpt: Data-efficient adaptation of pretrained language models for image captioning. In *Proceedings of the IEEE/CVF conference on computer vision and pattern recognition*, 18030–18040.

Cheng, K.; Sun, Q.; Chu, Y.; Xu, F.; YanTao, L.; Zhang, J.; and Wu, Z. 2024. SeeClick: Harnessing GUI Grounding for Advanced Visual GUI Agents. In *Proceedings of the 62nd Annual Meeting of the Association for Computational Linguistics (Volume 1: Long Papers)*, 9313–9332.

Duan, H.; Yang, J.; Qiao, Y.; Fang, X.; Chen, L.; Liu, Y.; Dong, X.; Zang, Y.; Zhang, P.; Wang, J.; et al. 2024. Vlmevalkit: An open-source toolkit for evaluating large multi-modality models. In *Proceedings of the 32nd ACM international conference on multimedia*, 11198–11201.

Fu, X.; Hu, Y.; Li, B.; Feng, Y.; Wang, H.; Lin, X.; Roth, D.; Smith, N. A.; Ma, W.-C.; and Krishna, R. 2024. Blink: Multimodal large language models can see but not perceive. In *European Conference on Computer Vision*, 148–166. Springer.

Guan, T.; Liu, F.; Wu, X.; Xian, R.; Li, Z.; Liu, X.; Wang, X.; Chen, L.; Huang, F.; Yacoob, Y.; et al. 2024. Hallusion-bench: an advanced diagnostic suite for entangled language hallucination and visual illusion in large vision-language models. In *Proceedings of the IEEE/CVF Conference on Computer Vision and Pattern Recognition*, 14375–14385.

Guo, Q.; De Mello, S.; Yin, H.; Byeon, W.; Cheung, K. C.; Yu, Y.; Luo, P.; and Liu, S. 2024. Regiongpt: Towards region understanding vision language model. In *Proceedings of the IEEE/CVF Conference on Computer Vision and Pattern Recognition*, 13796–13806.

Huang, S.; Dong, L.; Wang, W.; Hao, Y.; Singhal, S.; Ma, S.; Lv, T.; Cui, L.; Mohammed, O. K.; Patra, B.; Liu, Q.; Aggarwal, K.; Chi, Z.; Bjorck, N.; Chaudhary, V.; Som, S.; SONG, X.; and Wei, F. 2023. Language Is Not All You Need: Aligning Perception with Language Models. In Oh, A.; Naumann, T.; Globerson, A.; Saenko, K.; Hardt, M.; and Levine, S., eds., *Advances in Neural Information Processing Systems*, volume 36, 72096–72109. Curran Associates, Inc.

Kazemzadeh, S.; Ordonez, V.; Matten, M.; and Berg, T. 2014. ReferItGame: Referring to objects in photographs of natural scenes. In *Proceedings of the 2014 conference on empirical methods in natural language processing (EMNLP)*, 787–798.

Kosti, R.; Alvarez, J. M.; Recasens, A.; and Lapedriza, A. 2020. Context Based Emotion Recognition Using EMOTIC Dataset. *IEEE Transactions on Pattern Analysis and Machine Intelligence*, 42(11): 2755–2766.

Li, F.; Hogg, D. C.; and Cohn, A. G. 2024. Reframing Spatial Reasoning Evaluation in Language Models: A Real-World Simulation Benchmark for Qualitative Reasoning. In Larson, K., ed., *Proceedings of the Thirty-Third International Joint Conference on Artificial Intelligence, IJCAI-24*, 6342–6349. International Joint Conferences on Artificial Intelligence Organization. Main Track.

Li, J.; Li, D.; Savarese, S.; and Hoi, S. 2023. Blip-2: Bootstrapping language-image pre-training with frozen image encoders and large language models. In *International conference on machine learning*, 19730–19742. PMLR.

Li, Y.; Huang, H.; Chen, C.; Huang, K.; Huang, C.; and Zhiyuan Liu, Z. G.; Xu, J.; Li, Y.; Li, R.; and Sun, M. 2025. Magician: Revealing the Magic of Free-Form Multi-Image Grounding in Multimodal Large Language Models. arXiv:2501.05767.

Lin, T.-Y.; Maire, M.; Belongie, S.; Hays, J.; Perona, P.; Ramanan, D.; Dollár, P.; and Zitnick, C. L. 2014. Microsoft COCO: Common objects in context. In *European Conference on Computer Vision*, 740–755.

Liu, H.; Li, C.; Wu, Q.; and Lee, Y. J. 2023. Visual Instruction Tuning. In Oh, A.; Naumann, T.; Globerson, A.; Saenko, K.; Hardt, M.; and Levine, S., eds., *Advances in Neural Information Processing Systems*, volume 36, 34892–34916. Curran Associates, Inc.

Liu, Y.; Duan, H.; Zhang, Y.; Li, B.; Zhang, S.; Zhao, W.; Yuan, Y.; Wang, J.; He, C.; Liu, Z.; et al. 2024. Mmbench: Is your multi-modal model an all-around player? In *European conference on computer vision*, 216–233. Springer.

Meng, F.; Li, C.; Wang, J.; Lu, Q.; Tian, H.; Yang, T.; Liao, J.; Zhu, X.; Dai, J.; Qiao, Y.; et al. 2025. MMU: Multimodal Multi-image Understanding for Evaluating Large Vision-Language Models. In *The Thirteenth International Conference on Learning Representations*.

Neuhold, G.; Ollmann, T.; Rota Bulo, S.; and Kortschieder, P. 2017. The mapillary vistas dataset for semantic understanding of street scenes. In *Proceedings of the IEEE international conference on computer vision*, 4990–4999.

Nir, G.; Hor, S.; Karimi, D.; Fazli, L.; Skinnider, B. F.; Tavassoli, P.; Turbin, D.; Villamil, C. F.; Wang, G.; Wilson, R. S.; et al. 2018. Automatic grading of prostate cancer in digitized histopathology images: Learning from multiple experts. *Medical image analysis*, 50: 167–180.

OpenAI. 2023. GPT-4V(ision) system card. <https://openai.com/index/gpt-4v-system-card/>. Accessed: 2023.

OpenAI. 2024. Hello GPT-4o. <https://openai.com/index/hello-gpt-4o/>. Accessed: 2024.

Rasheed, H.; Maaz, M.; Shaji, S.; Shaker, A.; Khan, S.; Cholakkal, H.; Anwer, R. M.; Xing, E.; Yang, M.-H.; and Khan, F. S. 2024. Glamm: Pixel grounding large multimodal model. In *Proceedings of the IEEE/CVF Conference on Computer Vision and Pattern Recognition*, 13009–13018.

Stirenko, S.; Kochura, Y.; Alienin, O.; Rokovy, O.; Gordienko, Y.; Gang, P.; and Zeng, W. 2018. Chest X-Ray Analysis of Tuberculosis by Deep Learning with Segmentation and Augmentation. In *2018 IEEE 38th International Conference on Electronics and Nanotechnology (ELNANO)*, 422–428.

Wang, P.; Bai, S.; Tan, S.; Wang, S.; Fan, Z.; Bai, J.; Chen, K.; Liu, X.; Wang, J.; Ge, W.; Fan, Y.; Dang, K.; Du, M.; Ren, X.; Men, R.; Liu, D.; Zhou, C.; Zhou, J.; and Lin, J. 2024a. Qwen2-VL: Enhancing Vision-Language Model’s Perception of the World at Any Resolution. arXiv:2409.12191.

Wang, W.; Shi, M.; Li, Q.; Wang, W.; Huang, Z.; Xing, L.; Chen, Z.; Li, H.; Zhu, X.; Cao, Z.; Chen, Y.; Lu, T.; Dai, J.; and Qiao, Y. 2024b. The All-Seeing Project: Towards Panoptic Visual Recognition and Understanding of the Open World. In *The Twelfth International Conference on Learning Representations*.

Wei, F.; Zhao, J.; Yan, K.; Zhang, H.; and Xu, C. 2024. A large-scale human-centric benchmark for referring expression comprehension in the LMM era. In *Proceedings of the 38th International Conference on Neural Information Processing Systems*, 69566–69587.

Wu, M.; Cai, X.; Ji, J.; Li, J.; Huang, O.; Luo, G.; Fei, H.; Jiang, G.; Sun, X.; and Ji, R. 2024. ControlMLM: Training-Free Visual Prompt Learning for Multi-modal Large Language Models. In Globerson, A.; Mackey, L.; Belgrave, D.; Fan, A.; Paquet, U.; Tomczak, J.; and Zhang, C., eds., *Advances in Neural Information Processing Systems*, volume 37, 45206–45234. Curran Associates, Inc.

Yang, J.; Ang, Y. Z.; Guo, Z.; Zhou, K.; Zhang, W.; and Liu, Z. 2022. Panoptic scene graph generation. In *European conference on computer vision*, 178–196. Springer.

Yang, J.; Zhang, H.; Li, F.; Zou, X.; Li, C.; and Gao, J. 2023. Set-of-Mark Prompting Unleashes Extraordinary Visual Grounding in GPT-4V. arXiv:2310.11441.

Ying, K.; Meng, F.; Wang, J.; Li, Z.; Lin, H.; Yang, Y.; Zhang, H.; Zhang, W.; Lin, Y.; Liu, S.; et al. 2024. MMT-Bench: A Comprehensive Multimodal Benchmark for Evaluating Large Vision-Language Models Towards Multitask AGI. In *International Conference on Machine Learning*, 57116–57198. PMLR.

Yu, W.; Yang, Z.; Li, L.; Wang, J.; Lin, K.; Liu, Z.; Wang, X.; and Wang, L. 2024. MM-Vet: Evaluating Large Multi-modal Models for Integrated Capabilities. In *International Conference on Machine Learning*, 57730–57754. PMLR.

Yue, X.; Ni, Y.; Zhang, K.; Zheng, T.; Liu, R.; Zhang, G.; Stevens, S.; Jiang, D.; Ren, W.; Sun, Y.; et al. 2024. Mmmu: A massive multi-discipline multimodal understanding and reasoning benchmark for expert agi. In *Proceedings of the IEEE/CVF Conference on Computer Vision and Pattern Recognition*, 9556–9567.

Zhang, H.; Li, H.; Li, F.; Ren, T.; Zou, X.; Liu, S.; Huang, S.; Gao, J.; Leizhang; Li, C.; et al. 2024a. Llava-grounding: Grounded visual chat with large multimodal models. In *European Conference on Computer Vision*, 19–35. Springer.

Zhang, Q.; Wang, Z.; Zhang, D.; Niu, W.; Caldwell, S.; Gedeon, T.; Liu, Y.; and Qin, Z. 2024b. Visual Prompting in LLMs for Enhancing Emotion Recognition. In *Proceedings of the 2024 Conference on Empirical Methods in Natural Language Processing*, 4484–4499.

Zhang, S.; Huang, D.; Deng, J.; Tang, S.; Ouyang, W.; He, T.; and Zhang, Y. 2024c. Agent3d-zero: An agent for zero-shot 3d understanding. In *European Conference on Computer Vision*, 186–202. Springer.

Zhou, S.; Chang, H.; Jiang, S.; Fan, Z.; Zhu, Z.; Xu, D.; Chari, P.; You, S.; Wang, Z.; and Kadambi, A. 2024a. Feature 3dgs: Supercharging 3d gaussian splatting to enable distilled feature fields. In *Proceedings of the IEEE/CVF Conference on Computer Vision and Pattern Recognition*, 21676–21685.

Zhou, X.; Ran, X.; Xiong, Y.; He, J.; Lin, Z.; Wang, Y.; Sun, D.; and Yang, M.-H. 2024b. GALA3D: Towards Text-to-3D Complex Scene Generation via Layout-guided Generative Gaussian Splatting. In *International Conference on Machine Learning*, 62108–62118. PMLR.

## Appendix

```
[  
  {  
    "meta_source": "Where is this data  
      retrieved?",  
    "data_file": "specify your respective separate  
      data file name",  
    "region": [  
      {  
        "meta_bbox": ["x1", "y1", "x2", "y2"],  
        "meta_polygon": "segmentation mask in  
          polygon format",  
        "meta_annotation": "original data annotation",  
        "question": "What does <VP> denote a region?",  
        "answer": "Propose a Q-A answer."  
      }  
    ]  
  ]  
]
```

Table 7: The example of the metadata.

## Benchmark Curation

We propose a benchmark consisting of two evaluation stages. To accurately achieve the goals of each stage, we collected data separately for stages 1 and 2 and defined a unified data-generation and review pipeline as in Figures 3 and 4. In both stages, these pipelines follow five phases: raw data collection, data-quality assessment, question definition, QA generation, and visual-prompt (VP) rendering. Below, we describe each phase in detail.

### Stage 1 Data Curation

**Question Definition.** The objective of Stage 1 is to evaluate how the model perceives VPs. To this end, we define four core aspects of VP perception: *existence*, *enumeration*, *location*, and *reference*. Specifically:

1. **Existence.** “Does a VP of this particular color and shape appear in the image or not?”
2. **Enumeration.** “How many VPs of this specific shape are present in the image?”
3. **Location.** “What is the position (e.g., top-left, bottom-right) of a given VP in the image?”
4. **Reference.** “Which object is being highlighted by the VP in the image?”

**Data Collection.** The dataset must support all four question types, so we chose an object-detection or semantic segmentation dataset. To minimize domain shift, letting the model focus on VP perception, we selected MS-COCO (Lin et al. 2014), which is widely used as pretraining data for multimodal LLMs.

**QA Generation.** Questions need to accurately reflect the four defined intents, and answers must be exact. We created

VP Shape	Context
Tag	A tag is a small label located at the center of a target, displaying a number or letter. It may be in red, blue, green, or black, and can be circular or square in shape.
Bounding Box	A bounding box is a rectangular frame that marks a target, which may be in red, blue, green, or black.
Arrow	An arrow is a symbol that points to a target, which may be in red, blue, green, or black.
Mask	A mask is a filled area used to indicate a target region, which may be in red, blue, green, or black.
Contour	A contour is the outline of a target, which may be in red, blue, green, or black. It can be drawn precisely along the outline or may resemble a loosely hand-drawn line.
Oval	An oval is an elliptical shape that encircles a target, which may be in red, blue, green, or black.
Point	A point is a square or circular dot that represents a target, located at the center of the marked target, which may be in red, blue, green, or black.
Scribble	A scribble is a random hand-drawn line that indicates a target, which may be in red, blue, green, or black.

Table 8: The Description of Visual Prompt Shapes.

Question Types	Question Template
Existence	Is there any <VP> in the image?
Enumeration	How many <color> <VP> are in the image?
Location	Where is the <color> <VP> located in the image?
Reference	What is the <color> <VP> referring to in the image?

Table 9: Stage 1 question types and their corresponding templates.

templates for each question–answer pair in Table 9. To make them read more fluently, we used a large language model to rephrase both questions and answers.

**VP Rendering.** To generate diverse VPs, we developed a modular rendering framework. It supports many VP shapes by using the factory pattern in the core visualization module and the proxy pattern at the interface layer. Our implementation defines 8 independent VP-shape classes; new shapes can be added without altering existing code. We integrate this into our data pipeline via a unified drawing interface with customizable attributes, improving readability and reducing development effort.

### Stage 2 Data Curation

**Question Definition.** Stage 2 examines how different VPs affect downstream tasks. We selected six common tasks that also involve reference information:

1. Medical Image Analysis (MIA),

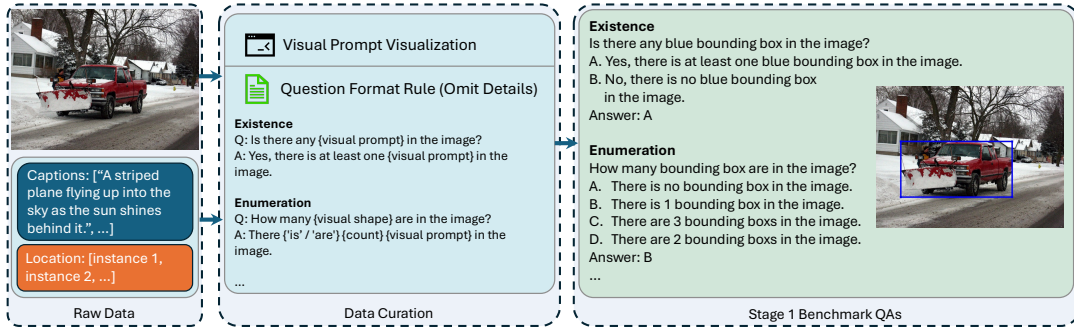


Figure 3: Benchmark Stage 1 Q&As generation pipeline.

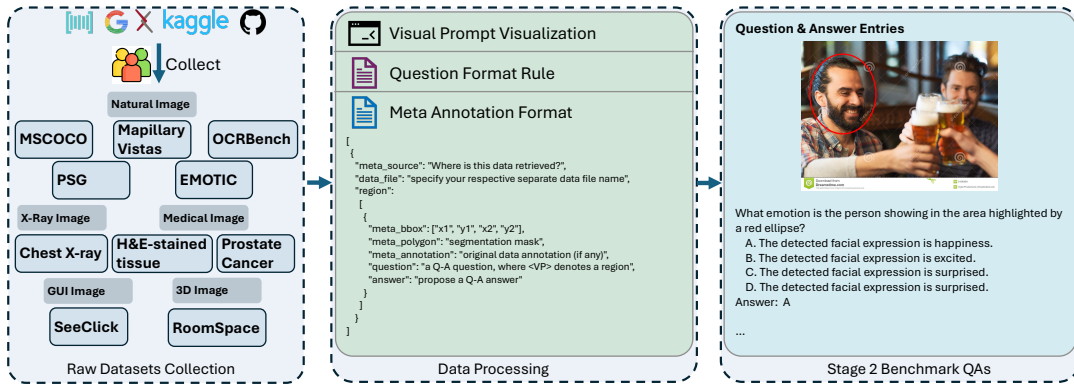


Figure 4: Benchmark Stage 2 Q&As generation pipeline.

2. Indoor 3D Object Recognition,
3. Facial Expression Recognition,
4. Street-Scene Recognition,
5. GUI Element Recognition,
6. Scene-Graph Generation (SGG).

For each task, we retain its original objective. For example, in medical-image analysis, the question becomes: “Identify the region highlighted by the VP and diagnose the possible condition.”

**Data Collection.** Each co-author was assigned one downstream task and located the corresponding training or validation dataset by: (i) original publication datasets, those introduced by the task’s authors; (ii) public repositories, any relevant dataset on HuggingFace\*, Papers with Code†, etc. Each dataset then reviewed by three independent examiners (excluding its collector) to ensure:

1. license availability, usable under our intended license,
2. VP applicability, supports overlaying visual prompts,
3. annotation quality, those clear, accurate labels to avoid ambiguous or incorrect QAs.

Approved datasets were converted into the metadata schema defined in Table 7.

\*<https://huggingface.co/>

†<https://paperswithcode.com/>

**QA Generation.** To ensure consistency and clarity, we designed standardized question templates tailored to each task. For example, in the facial emotion recognition task, the template takes the form:

*What emotion is the person showing in the area highlighted by a red ellipse?*

To generate natural distractors, we randomly selected three incorrect emotion categories from the dataset and prompted the LLM to produce three fluent but misleading alternatives.

For the MIA (Medical Image Analysis) task, the template follows a similar pattern:

*A <Medical Image Type> of <Human Organ> is provided, with the region of interest marked by <color> <VP>. Please assess the pathological characteristics of this region.*

Here, distractors were generated by providing the LLM with incorrect tissue types and unrelated disease causes to construct plausible but incorrect options.

Likewise, in the SVR (Street-View Recognition) task, the question format is:

*What does the red oval highlight in this <color> <VP>?*

The LLM was guided using unrelated traffic components as cues, ensuring the distractors appeared contextually relevant but remained distinguishable from the correct answer.

Scenario	Question Template
FER	What emotion is the person showing in the area highlighted by <color> <VP>?
SVR	What does the red oval highlight in this <color> <VP>?
MIA	A <Medical Image Type> of <Human Organ> is provided, with the region of interest marked by <color> <VP>. Please assess the pathological characteristics of this region.
3DOR	Given a top-down and a front view (from south to north) of a room, identify the object marked by the <color> <VP> and specify its position.
SGG	What is the object that is on the thing highlighted by the <color> <VP>?
GUIER	Can you recognize the graphical user interface (GUI) element highlighted by the <color> <VP>?

Table 10: Stage 2 downstream-task question templates: Facial Emotion Recognition (FER), Street-view Recognition (SVR), Medical Image Analysis (MIA), 3D Object Recognition (3DOR), Scene-Graph Generation (SGG), and GUI Element Recognition (GUIER).

**VP Rendering.** Thanks to the Stage 1 framework, we simply reused the same codebase to render the visual prompts needed for Stage 2.

Model	Avg. VP Accuracy	Avg. Downstream Accuracy
Human Baseline	90.03	-
GPT-4o (proprietary)	68.80	72.56
Qwen-VL-Max (proprietary)	82.63	75.61
Qwen2.5-VL-3B	73.41	65.76
Qwen2.5-VL-7B	81.29	69.08
Qwen2.5-VL-32B	83.22	70.93
Qwen2.5-VL-72B	82.80	75.55
InternVL3-1B	71.46	55.98
InternVL3-8B	84.11	72.89
InternVL3-38B	86.89	77.17
InternVL3-78B	<b>87.97</b>	<b>79.05</b>
Molmo-72B	85.61	76.18
NVLM-D-72B	85.39	74.67

Table 11: Simplified summary of model scale versus VP perception (Stage 1) and downstream task accuracy (Stage 2).

## More Experiments Results and Analysis

All experiments were conducted on a cluster of 8×H800 GPUs (80 GB memory each). As no training was performed, the computational cost is limited to model inference. During inference, the decoding was restricted to the top-1 response for all evaluations to eliminate randomness.

**Human performance baseline compared with model results.** To establish a human performance baseline, participants unfamiliar with this work individually completed the Stage 1 benchmark. For efficiency, 1,000 questions were randomly sampled from the original dataset, and each participant took the test independently without any prior briefing or in-process discussion.

Human participants achieved an average accuracy of 90.03% across all tasks, whereas the best-performing model, InternVL3-78B, reached 87.97%. This indicates that while current models exhibit near-human VP perception, there remains room for improvement. In certain VP types, however, the model surpassed human performance; for example, InternVL3-78B achieved 93.87% on **Tag**, exceeding the human score of 89.00%. Nevertheless, model stability lagged behind that of humans. In **Point** perception, for instance, human accuracy was 90.68%, whereas model performance ranged from 49.28% to 81.59%.

**Open-source models have already overtaken proprietary models in VP perception.** In Table 13, most tested open-source models achieve an average accuracy of around 80%, with InternVL3-78B reaching 88.62%. By contrast, proprietary models score 68.93% for GPT-4o, 72.13% for Doubao-Seed-1.6, and 83.7% for Qwen-VL-Max. Surprisingly, GPT-4o’s spatial perception of VPs lags considerably, at only 57.83% accuracy. In our Stage 2 evaluation on downstream tasks, NVLM-D-72B, Qwen-2.5-VL-72B, InternVL3-78B, and Molmo-72B perform very competitively against proprietary models. Notably, Molmo-72B outperforms GPT-4o on MIA, street-view recognition, 3D object recognition, and SGG tasks. Taken together, these findings indicate that open-source MLLMs are not only closing the gap but have already surpassed proprietary counterparts in VP perception and several downstream domains.

**Model scale strongly correlates with VP perception accuracy.** As shown in Table 11, both the Qwen2.5-VL and InternVL3 families exhibit consistent performance gains with increasing parameter size, with InternVL3-78B achieving the highest Stage 1 accuracy 87.97%. Larger models demonstrate particular advantages on irregular VP types such as Mask and Point, where smaller models show pronounced drops, suggesting that fine-grained regional perception benefits from higher-capacity vision–language representations. For Stage 2 downstream tasks: models above 30B parameters, including InternVL3-38B, InternVL3-78B, Molmo-72B, and NVLM-D-72B, consistently outperform mid- and small-scale counterparts across MIA, 3D object recognition, and street-view recognition. These results indicate that scaling improves both VP detection and the integration of VP cues into task-specific reasoning, narrowing the gap to human-level performance and enabling robust transfer to diverse application domains.

## Prompts

Accurate prompt design is critical for consistent data generation, annotation refinement, and model evaluation in VP-Bench. This section details the prompt templates used across three stages of the pipeline. First, Table 14 presents the multi-choice question generation prompt, which instructs the LLM to produce plausible but incorrect distractors to enhance dataset diversity. Second, Table 15 shows the annotation expansion prompt, which rephrases and reorganizes textual descriptions while retaining their core semantics to improve linguistic variety. Finally, Tables 16 and 17 describe the benchmarking prompts that standardize model evaluation using a consistent question–answering format, with or

Model	Emotic		Mapillary Vistas		MIA		SD-100		SGG		See-Click		Avg. Vis. ( $\Delta$ )	Avg. Txt.
	Vis.	Txt.	Vis.	Txt.	Vis.	Txt.	Vis.	Txt.	Vis.	Txt.	Vis.	Txt.		
CogVLM2-LLama3-Chat-19B	70.71	78.12	33.49	23.92	5.40	5.60	31.33	13.33	83.30	83.30	75.31	43.50	49.92 (+8.86)	41.30
DeepSeek-VL2	20.90	67.76	24.88	24.40	20.90	20.60	45.67	19.33	83.30	84.37	67.50	68.00	43.86 (-3.55)	47.41
GLM-4V-9B	64.94	69.88	53.59	30.62	18.19	18.70	59.33	40.00	86.32	86.59	96.25	95.00	63.10 (+6.31)	56.80
Llama-3.2-90B-Vision-Instruct	65.65	69.65	51.20	44.98	59.50	62.70	58.00	56.00	88.99	92.18	98.50	97.50	70.31 (-0.20)	70.50
LLaVA-OneVision-Qwen2-7B-OV-HF	64.39	74.29	47.37	33.49	16.72	17.72	63.67	63.33	92.01	90.76	92.01	94.25	62.70 (+0.39)	62.31
LLaVA-v1.6-34B-HF	64.05	64.47	48.33	43.06	37.60	35.30	52.33	55.00	91.30	89.52	96.30	94.75	64.99 (+1.30)	63.68
MiniCPM-V-2.6	67.06	72.71	26.32	35.41	15.30	13.70	38.00	65.33	89.08	89.88	92.75	96.75	54.75 (-7.55)	62.30
Molmo-72B-0924	67.38	61.88	60.77	52.15	62.80	62.90	78.00	67.33	91.83	86.59	96.30	89.75	76.18 (+6.08)	70.10
NVLM-D-72B	72.71	73.18	49.76	41.15	58.10	60.90	77.00	75.67	93.43	92.18	97.00	96.75	74.67 (+1.36)	73.31
Ovis2-34B	73.10	74.12	50.72	60.77	37.30	50.20	83.33	79.00	94.58	92.36	99.69	99.25	73.12 (-2.83)	75.95
Qwen2.5-VL-72B	71.43	71.53	61.72	59.81	43.80	39.20	83.33	85.67	95.47	94.14	97.53	98.00	75.55 (+0.82)	74.73

Table 12: Comparison of model performance with VP and text-based spatial prompt (TP) baseline on Stage 2 evaluation. Average VP accuracy reports absolute accuracy followed by the signed changed  $\Delta$  relative to its baseline.

Model	Visual Prompt Types									Problem Types				Avg.
	Tag	Arrow	BBox	Contour	Mask	Oval	Point	Scribble	Enumeration	Existence	Rough-Loc.	VP-Ref.		
<i>Human Baseline</i>														
Human Reviewers	89.00	92.62	97.29	87.68	85.28	94.87	90.68	82.80	90.73	94.36	97.68	84.26	90.03	
<i>Proprietary Models</i>														
GPT-4o	69.95	70.27	74.18	77.18	65.32	79.77	49.28	64.45	60.44	87.03	57.83	67.74	68.80	
Doubao-Seed-1.6	86.21	79.60	93.60	72.43	71.19	50.17	47.49	62.30	62.47	64.04	95.34	80.53	70.37	
Qwen-VL-Max	92.27	82.84	93.10	88.75	67.51	92.84	69.31	74.45	81.80	88.11	92.13	76.82	82.63	
<i>Pre-trained Models</i>														
Qwen2.5-VL-72B-Instruct	92.26	82.57	92.88	88.62	68.68	92.83	69.58	74.77	81.84	88.26	92.01	75.79	82.80	
NVLM-D-72B	91.28	88.23	91.60	90.22	76.02	93.35	77.00	75.41	83.82	93.99	92.06	76.50	85.39	
Molmo-72B-0924	90.71	85.31	92.92	89.61	79.05	93.18	76.57	77.56	87.18	97.24	92.46	70.08	85.61	
InternVL3-78B	93.87	85.77	94.25	91.56	80.01	95.81	81.59	80.89	88.59	92.93	95.24	79.65	87.97	

Table 13: Performance on VP-shape and question-type subtasks, sorted by overall accuracy.

without explicit VP descriptions, enabling controlled experiments on VP perception.

## Visual Prompt Properties

Visual prompts are visual cues embedded within images that help guide a model’s attention and interpretation. They come in a variety of shapes, such as tags, bounding boxes, arrows, masks, contours, ovals, points, and scribbles, each designed with distinct properties. These properties include color variations, line styles, thicknesses, and additional stylistic features that can be adjusted to enhance contrast and clarity. Table 18 provides a detailed overview of these visual prompt shapes along with a set of attributes for each, illustrating the customizable nature of these prompts and how they can be tailored for specific applications.

## Qualitative Result

In this section, we present qualitative visual results from our evaluation. In Stage 1, we assess the model’s performance across all eight visual prompt types and five question types. Representative examples, illustrated in Figures 5, 6, 7, 8, 9, 10, 11, and 12, demonstrate how models interpret and respond to varied VPs. In Stage 2, we showcase qualitative results for downstream tasks, as shown in Figures 13, 14, and 15, where model responses to task-specific questions are examined. These results provide key insights into the models’ capabilities in processing multimodal inputs and highlight areas for further improvement.

<SYSTEM PROMPT>

You are an AI assistant specialized in generating plausible distractor options for multiple-choice visual questions. Your primary task is to create distractor options that are incorrect but plausible, aiming to challenge the user while ensuring it remains distinguishable from the correct answer.

<USER PROMPT>

For the question ‘<question>’ and its correct answer ‘<answer>’, generate three plausible but incorrect distractor options. These options should be similar to the correct answer to create confusion, yet still distinct enough to be clearly wrong.

Your output should be formatted as follows in JSON: ` ` ` json

```
{
  "distractor_options": [
    "Distractor option 1",
    "Distractor option 2",
    "Distractor option 3"
  ]
}
``
```

Table 14: Prompt template used to instruct the LLM to generate plausible but incorrect distractor options for multiple-choice visual questions. The system prompt defines the task, while the user prompt supplies the question and the correct answer.

---

The following paragraph should be rewritten while retaining the essential information. Different expressions should be used, and the paragraph may be reorganized if necessary. The paragraph should not be altered merely by converting the passive voice to active voice or vice versa.

---

Table 15: Instruction template for rewriting a paragraph while preserving its essential information. The guidance emphasizes using different expressions and allows reorganization of the content rather than simply switching between passive and active voice.

---

Context: {VP description}  
 {QUESTION}  
 A. {OPTION\_A}  
 B. {OPTION\_B}  
 C. {OPTION\_C}  
 D. {OPTION\_D}

---

Answer with the option's letter from the given choices directly.

---

Table 16: General instruction prompt template used to generate multiple-choice questions for VP perception tasks. The {VP description} field is optionally included depending on the experimental setting.

<i>Example with VP description</i>	<i>Example without VP description</i>
<p>Context: An arrow is a symbol that points to a target, which may be in red, blue, green, or black.</p> <p>Where is the red arrow located in the image?</p> <p>A. The red arrow is located in the bottom-left.    B. The red arrow is located in the bottom-right.    C. The red arrow is located in the top-right.    D. The red arrow is located in the top-left.</p> <p>Answer with the option's letter from the given choices directly.</p>	<p>Where is the red arrow located in the image?</p> <p>A. The red arrow is located in the bottom-left.    B. The red arrow is located in the bottom-right.    C. The red arrow is located in the top-right.    D. The red arrow is located in the top-left.</p> <p>Answer with the option's letter from the given choices directly.</p>

Table 17: Comparison of instruction arrangements with and without a VP description. Left: Guiding the model to interpret the visual prompt via the VP description; Right: Testing the model's ability to infer VP meaning from visual cues alone.

Visual Prompt Shape	Attribute 1	Attribute 2	Attribute 3	Attribute 4	Attribute 5
Tag	Red Color Tag	Blue Color Tag	Green Color Tag	Black Color Tag	Background Contrastive Color Tag
	Alphabet	Digit			
	Square	Round			
Bounding Box	Small Front	Medium Front	Big Front	Black Color Line	Background Contrastive Color Line
	Red Color Line	Blue Color Line	Green Color Line	Black Color Line	Background Contrastive Color Line
	Thin Line	Normal Width Line	Thick Line		
Arrow	Vertex No Shape	Vertex Square Shape	Vertex Round Shape	Black Color Line	Background Contrastive Color Line
	Red Color Line	Blue Color Line	Green Color Line	Black Color Line	Background Contrastive Color Line
	Thin Line	Normal Width Line	Thick Line		
Mask	Arrow Bold Style	Arrow Thin Style	Blue Color Line (Filled)	Green Color Line (Filled)	Black Color Line (Filled)
	Red Color Line (Filled)	Blue Color Line (Filled)	Green Color Line (Filled)	Black Color Line (Filled)	Background Contrastive Color Line (Filled)
	Thin Line	Normal Width Line	Thick Line		
Contour	Contour with Filled	Contour Only	Blue Color Line	Green Color Line	Black Color Line
	Red Color Line	Blue Color Line	Green Color Line	Black Color Line	Background Contrastive Color Line
	Thin Line	Normal Width Line	Thick Line		
Oval	Strict Contour	Loosen Contour	Blue Color Line	Green Color Line	Black Color Line
	Red Color Line	Blue Color Line	Green Color Line	Black Color Line	Background Contrastive Color Line
	Thin Line	Normal Width Line	Thick Line		
Point	Red Color Dot	Blue Color Dot	Green Color Dot	Black Color Dot	Background Contrastive Color Dot
	Small Size	Medium Size	Big Size		
	Round Shape	Square Shape	Blue Color Line	Green Color Line	Background Contrastive Color Line
Scribble	Red Color Line	Blue Color Line	Green Color Line	Black Color Line	Background Contrastive Color Line
	Thin Line	Normal Width Line	Thick Line		

Table 18: Visual prompt shapes and their attributes.

**Arrow – Enumeration**

Question: How many arrow are in the image?  
=====

Options  
A. There is 1 arrow in the image.  
B. There are 2 arrows in the image.  
C. There is no arrow in the image.  
D. There are 3 arrows in the image.  
=====

Answer: A

Qwen2.5-VL-72B: A

**Arrow – Enumeration**

Question: How many arrow are in the image?  
=====

Options  
A. There are 3 arrows in the image.  
B. There is 1 arrow in the image.  
C. There is no arrow in the image.  
D. There are 2 arrows in the image.  
=====

Answer: B

Qwen2.5-VL-72B: C

**Arrow – Existence**

Question: Is there any arrow in the image?  
=====

Options  
A. No, there is no arrow in the image.  
B. Yes, there is at least one arrow in the image.  
=====

Answer: B

InternVL2.5-78B: B

**Arrow – Existence**

Question: Is there any arrow in the image?  
=====

Options  
A. No, there is no tag in the image.  
B. Yes, there is at least one tag in the image.  
=====

Answer: A

InternVL2.5-78B: B

**Arrow – Location**

Question: Where is the blue arrow located in the image?  
=====

Options  
A. The blue arrow is located in the right-half.  
B. The blue arrow is located in the bottom-half.  
C. The blue arrow is located in the left-half.  
D. The blue arrow is located in the top-half.  
=====

Answer: C

Qwen2.5-VL-72B: C

**Arrow – Location**

Question: Where is the blue arrow located in the image?  
=====

Options  
A. The blue arrow is located in the left-half.  
B. The blue arrow is located in the bottom-half.  
C. The blue arrow is located in the top-half.  
D. The blue arrow is located in the right-half.  
=====

Answer: A

Qwen2.5-VL-72B: B

**Arrow – Reference**

Question: What is the green arrow referring to in the image?  
=====

Options  
A. The green arrow refers to a laptop.  
B. The green arrow refers to a drink.  
C. The green arrow refers to a person.  
D. The green arrow refers to a book.  
=====

Answer: C

DeepSeek-VL2: C

**Arrow – Reference**

Question: What is the black arrow referring to in the image?  
=====

Options  
A. The black arrow refers to a line on the grass.  
B. The black arrow refers to a shadow on the ground.  
C. The black arrow refers to a person.  
D. The black arrow refers to a baseball glove.  
=====

Answer: C

DeepSeek-VL2: B

Figure 5: Qualitative results of arrow shape in Stage 1 evaluation.

**Bounding Box – Enumeration**

Question: How many bounding box are in the image?  
=====

Options

A. There is 1 bounding box in the image.  
B. There are 3 bounding boxes in the image.  
C. There is no bounding box in the image.  
D. There are 2 bounding boxes in the image.  
=====

Answer: A

✓
Qwen2.5-VL-72B: A

**Bounding Box – Enumeration**

Question: How many bounding box are in the image?  
=====

Options

A. There are 2 bounding boxes in the image.  
B. There is no bounding box in the image.  
C. There are 3 bounding boxes in the image.  
D. There is 1 bounding box in the image.  
=====

Answer: D

✗
Qwen2.5-VL-72B: B

**Bounding Box – Existence**

Question: Is there any bounding box in the image?  
=====

Options

A. No, there is no bounding box in the image.  
B. Yes, there is at least one bounding box in the image.  
=====

Answer: B

✓
InternVL2.5-78B: B

**Bounding Box – Existence**

Question: Is there any bounding box in the image?  
=====

Options

A. No, there is no bounding box in the image.  
B. Yes, there is at least one bounding box in the image.  
=====

Answer: B

✗
InternVL2.5-78B: A

**Bounding Box – Location**

Question: Where is the red bounding box located in the image?  
=====

Options

A. The red bounding box is located in the bottom-half.  
B. The red bounding box is located in the left-half.  
C. The red bounding box is located in the top-half.  
D. The red bounding box is located in the right-half.  
=====

Answer: D

✓
Qwen2.5-VL-72B: D

**Bounding Box – Location**

Question: Where is the blue bounding box located in the image?  
=====

Options

A. The blue bounding box is located in the top-half.  
B. The blue bounding box is located in the right-half.  
C. The blue bounding box is located in the left-half.  
D. The blue bounding box is located in the bottom-half.  
=====

Answer: D

✓
Qwen2.5-VL-72B: D

**Bounding Box – Reference**

Question: What is the blue bounding box referring to in the image?  
=====

Options

A. The blue bounding box refers to a car.  
B. The blue bounding box refers to a motorcycle.  
C. The blue bounding box refers to a scooter.  
D. The blue bounding box refers to a bicycle.  
=====

Answer: B

✓
DeepSeek-VL2: B

**Bounding Box – Reference**

Question: What is the blue bounding box referring to in the image?  
=====

Options

A. The blue bounding box refers to a wine glass.  
B. The blue bounding box refers to a bottle of wine.  
C. The blue bounding box refers to a kitchen utensil.  
D. The blue bounding box refers to a cup.  
=====

Answer: D

✗
DeepSeek-VL2: A

Figure 6: Qualitative results of bounding box shape in Stage 1 evaluation.

**Contour – Enumeration**

Question: How many contour are in the image?  
=====

Options  
A. There are 2 contours in the image.  
B. There is no contour in the image.  
C. There are 3 contours in the image.  
D. There is 1 contour in the image.  
=====

Answer: D

✓
Qwen2.5-VL-72B: D



**Contour – Enumeration**

Question: How many contour are in the image?  
=====

Options  
A. There are 3 contours in the image.  
B. There is no contour in the image.  
C. There are 2 contours in the image.  
D. There is 1 contour in the image.  
=====

Answer: D

✗
Qwen2.5-VL-72B: A



**Contour – Existence**

Question: Is there any contour in the image?  
=====

Options  
A. Yes, there is at least one contour in the image.  
B. No, there is no contour in the image.  
=====

Answer: A

✓
InternVL2.5-78B: A



**Contour – Existence**

Question: Is there any contour in the image?  
=====

Options  
A. Yes, there is at least one contour in the image.  
B. No, there is no contour in the image.  
=====

Answer: A

✗
InternVL2.5-78B: B



**Contour – Location**

Question: Where is the red contour located in the image?  
=====

Options  
A. The red contour is located in the right-half.  
B. The red contour is located in the top-half.  
C. The red contour is located in the left-half.  
D. The red contour is located in the bottom-half.  
=====

Answer: A

✓
Qwen2.5-VL-72B: A



**Contour – Location**

Question: Where is the green contour located in the image?  
=====

Options  
A. The green contour is located in the left-half.  
B. The green contour is located in the top-half.  
C. The green contour is located in the right-half.  
D. The green contour is located in the bottom-half.  
=====

Answer: A

✗
Qwen2.5-VL-72B: C



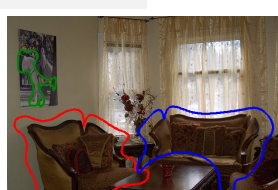
**Contour – Reference**

Question: What is the blue contour referring to in the image?  
=====

Options  
A. The blue contour refers to a coffee table.  
B. The blue contour refers to a chair.  
C. The blue contour refers to a couch.  
D. The blue contour refers to a vase.  
=====

Answer: C

✓
DeepSeek-VL2: C



**Contour – Reference**

Question: What is the red contour referring to in the image?  
=====

Options  
A. The red contour refers to a slice of cheese.  
B. The red contour refers to an apple.  
C. The red contour refers to a tomato.  
D. The red contour refers to a piece of bread.  
=====

Answer: B

✗
DeepSeek-VL2: C

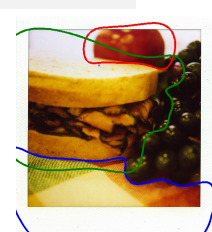


Figure 7: Qualitative results of contour shape in Stage 1 evaluation.

**Tag – Enumeration**

Question: How many tag are in the image?  
=====

Options  
A. There are 3 tags in the image.  
B. There is no tag in the image.  
C. There is 1 tag in the image.  
D. There are 2 tags in the image.  
=====

Answer: D

DeepSeek-VL2: C



**Tag – Enumeration**

Question: How many tag are in the image?  
=====

Options  
A. There is no tag in the image.  
B. There are 2 tags in the image.  
C. There are 3 tags in the image.  
D. There is 1 tag in the image.  
=====

Answer: D

InternVL2.5-78B: D



**Tag – Existence**

Question: Is there any tag in the image?  
=====

Options  
A. No, there is no tag in the image.  
B. Yes, there is at least one tag in the image.  
=====

Answer: B

InternVL2.5-78B: B



**Tag – Existence**

Question: Is there any tag in the image?  
=====

Options  
A. No, there is no tag in the image.  
B. Yes, there is at least one tag in the image.  
=====

Answer: A

Qwen2.5-VL-72B: B



**Tag – Location**

Question: Where is the red tag located in the image?  
=====

Options  
A. The red tag is located in the bottom-half.  
B. The red tag is located in the right-half.  
C. The red tag is located in the left-half.  
D. The red tag is located in the top-half.  
=====

Answer: C

Qwen2.5-VL-72B: C



**Tag – Location**

Question: Where is the black tag located in the image?  
=====

Options  
A. The black tag is located in the bottom-half.  
B. The black tag is located in the right-half.  
C. The black tag is located in the top-half.  
D. The black tag is located in the left-half.  
=====

Answer: B

Qwen2.5-VL-72B: D



**Tag – Reference**

Question: What is the blue tag referring to in the image?  
=====

Options  
A. The blue tag refers to a stovetop.  
B. The blue tag refers to a microwave.  
C. The blue tag refers to an oven.  
D. The blue tag refers to a dishwasher.  
=====

Answer: C

DeepSeek-VL2: C



**Tag – Reference**

Question: What is the blue tag referring to in the image?  
=====

Options  
A. The blue tag refers to a stovetop.  
B. The blue tag refers to a microwave.  
C. The blue tag refers to an oven.  
D. The blue tag refers to a dishwasher.  
=====

Answer: C

DeepSeek-VL2: B



Figure 8: Qualitative results of tag shape in Stage 1 evaluation.

**Mask – Enumeration**

Question: How many mask are in the image?  
=====

Options  
A. There are 2 masks in the image.  
B. There is no mask in the image.  
C. There are 3 masks in the image.  
D. There is 1 mask in the image.  
=====

Answer: D

✓
Qwen2.5-VL-72B: D

**Mask – Enumeration**

Question: How many mask are in the image?  
=====

Options  
A. There are 2 masks in the image.  
B. There is no mask in the image.  
C. There is 1 mask in the image.  
D. There are 3 masks in the image.  
=====

Answer: C

✗
Qwen2.5-VL-72B: B

**Mask – Existence**

Question: Is there any mask in the image?  
=====

Options  
A. Yes, there is at least one mask in the image.  
B. No, there is no mask in the image.  
=====

Answer: A

✓
InternVL2.5-78B: A

**Mask – Existence**

Question: Is there any mask in the image?  
=====

Options  
A. Yes, there is at least one mask in the image.  
B. No, there is no mask in the image.  
=====

Answer: A

✗
InternVL2.5-78B: B

**Mask – Location**

Question: Where is the black mask located in the image?  
=====

Options  
A. The black mask is located in the bottom-half.  
B. The black mask is located in the left-half.  
C. The black mask is located in the right-half.  
D. The black mask is located in the top-half.  
=====

Answer: C

✓
Qwen2.5-VL-72B: C

**Mask – Location**

Question: Where is the red mask located in the image?  
=====

Options  
A. The red mask is located in the right-half.  
B. The red mask is located in the top-half.  
C. The red mask is located in the left-half.  
D. The red mask is located in the bottom-half.  
=====

Answer: A

✗
Qwen2.5-VL-72B: B

**Mask – Reference**

Question: What is the red mask referring to in the image?  
=====

Options  
A. The red mask refers to a car.  
B. The red mask refers to a train.  
C. The red mask refers to a subway station.  
D. The red mask refers to a passenger bus.  
=====

Answer: B

✓
DeepSeek-VL2: B

**Mask – Reference**

Question: What is the black mask referring to in the image?  
=====

Options  
A. The black mask refers to a plate.  
B. The black mask refers to a napkin.  
C. The black mask refers to a fork.  
D. The black mask refers to a knife.  
=====

Answer: C

✗
DeepSeek-VL2: A

Figure 9: Qualitative results of mask shape in Stage 1 evaluation.

**Oval – Enumeration**

Question: How many oval are in the image?  
=====

Options

A. There is 1 oval in the image.  
B. There are 2 ovals in the image.  
C. There is no oval in the image.  
D. There are 3 ovals in the image.  
=====

Answer: A



✓
Qwen2.5-VL-72B: A

**Oval – Enumeration**

Question: How many oval are in the image?  
=====

Options

A. There is 1 oval in the image.  
B. There is no oval in the image.  
C. There are 2 ovals in the image.  
D. There are 3 ovals in the image.  
=====

Answer: A



✗
Qwen2.5-VL-72B: C

**Oval – Existence**

Question: Is there any oval in the image?  
=====

Options

A. Yes, there is at least one oval in the image.  
B. No, there is no oval in the image.  
=====

Answer: A



✓
InternVL2.5-78B: A

**Oval – Existence**

Question: Is there any oval in the image?  
=====

Options

A. Yes, there is at least one oval in the image.  
B. No, there is no oval in the image.  
=====

Answer: A



✗
InternVL2.5-78B: B

**Oval – Location**

Question: Where is the black oval located in the image?  
=====

Options

A. The black oval is located in the top-half.  
B. The black oval is located in the bottom-half.  
C. The black oval is located in the right-half.  
D. The black oval is located in the left-half.  
=====

Answer: D



✓
Qwen2.5-VL-72B: D

**Oval – Location**

Question: Where is the black oval located in the image?  
=====

Options

A. The black oval is located in the left-half.  
B. The black oval is located in the right-half.  
C. The black oval is located in the top-half.  
D. The black oval is located in the bottom-half.  
=====

Answer: D



✗
Qwen2.5-VL-72B: C

**Oval – Reference**

Question: What is the black oval referring to in the image?  
=====

Options

A. The black oval refers to a spaceship.  
B. The black oval refers to an airplane.  
C. The black oval refers to a drone.  
D. The black oval refers to a helicopter.  
=====

Answer: B



✓
DeepSeek-VL2: B

**Oval – Reference**

Question: What is the green oval referring to in the image?  
=====

Options

A. The green oval refers to a coffee table.  
B. The green oval refers to a bookshelf.  
C. The green oval refers to a dining table.  
D. The green oval refers to a sideboard.  
=====

Answer: C



✗
DeepSeek-VL2: D

Figure 10: Qualitative results of oval shape in Stage 1 evaluation.

**Scribble – Enumeration**

Question: How many scribbles are in the image?  
=====

Options  
A. There are 2 scribbles in the image.  
B. There is 1 scribble in the image.  
C. There are 3 scribbles in the image.  
D. There is no scribble in the image.  
=====

Answer: B

✓
Qwen2.5-VL-72B: B

**Scribble – Enumeration**

Question: How many scribbles are in the image?  
=====

Options  
A. There are 3 scribbles in the image.  
B. There is no scribble in the image.  
C. There are 2 scribbles in the image.  
D. There is 1 scribble in the image.  
=====

Answer: D

✗
Qwen2.5-VL-72B: C

**Scribble – Existence**

Question: Is there any scribble in the image?  
=====

Options  
A. No, there is no scribble in the image.  
B. Yes, there is at least one scribble in the image.  
=====

Answer: B

✓
InternVL2.5-78B: B

**Scribble – Existence**

Question: Is there any scribble in the image?  
=====

Options  
A. Yes, there is at least one scribble in the image.  
B. No, there is no scribble in the image.  
=====

Answer: A

✗
InternVL2.5-78B: B

**Scribble – Location**

Question: Where is the red scribble located in the image?  
=====

Options  
A. The red scribble is located in the left-half.  
B. The red scribble is located in the right-half.  
C. The red scribble is located in the bottom-half.  
D. The red scribble is located in the top-half.  
=====

Answer: A

✓
Qwen2.5-VL-72B: A

**Scribble – Location**

Question: Where is the red scribble located in the image?  
=====

Options  
A. The red scribble is located in the bottom-half.  
B. The red scribble is located in the right-half.  
C. The red scribble is located in the left-half.  
D. The red scribble is located in the top-half.  
=====

Answer: C

✗
Qwen2.5-VL-72B: A

**Scribble – Reference**

Question: Where is the red scribble located in the image?  
=====

Options  
A. The red scribble is located in the bottom-half.  
B. The red scribble is located in the right-half.  
C. The red scribble is located in the left-half.  
D. The red scribble is located in the top-half.  
=====

Answer: C

✓
DeepSeek-VL2: A

**Scribble – Reference**

Question: What is the green scribble referring to in the image?  
=====

Options  
A. The green scribble refers to a television remote.  
B. The green scribble refers to a video game controller.  
C. The green scribble refers to an electrical cord.  
D. The green scribble refers to a person.  
=====

Answer: D

✗
DeepSeek-VL2: B

Figure 11: Qualitative results of scribble shape in Stage 1 evaluation.

**Point – Enumeration**

Question: How many point are in the image?  
=====

Options  
A. There is no point in the image.  
B. There are 3 points in the image.  
C. There are 2 points in the image.  
D. There is 1 point in the image.  
=====

Answer: D

✓
Qwen2.5-VL-72B: D

**Point – Enumeration**

Question: How many point are in the image?  
=====

Options  
A. There are 2 points in the image.  
B. There are 3 points in the image.  
C. There is 1 point in the image.  
D. There is no point in the image.  
=====

Answer: C

✗
Qwen2.5-VL-72B: D

**Point – Existence**

Question: Is there any point in the image?  
=====

Options  
A. No, there is no point in the image.  
B. Yes, there is at least one point in the image.  
=====

Answer: B

✓
InternVL2.5-78B: B

**Point – Existence**

Question: Is there any point in the image?  
=====

Options  
A. Yes, there is at least one point in the image.  
B. No, there is no point in the image.  
=====

Answer: A

✗
InternVL2.5-78B: B

**Point – Location**

Question: Where is the black point located in the image?  
=====

Options  
A. The black point is located in the top-half.  
B. The black point is located in the bottom-half.  
C. The black point is located in the right-half.  
D. The black point is located in the left-half.  
=====

Answer: C

✓
Qwen2.5-VL-72B: C

**Point – Location**

Question: Where is the black point located in the image?  
=====

Options  
A. The black point is located in the bottom-half.  
B. The black point is located in the top-half.  
C. The black point is located in the left-half.  
D. The black point is located in the right-half.  
=====

Answer: D

✗
Qwen2.5-VL-72B: C

**Point – Reference**

Question: What is the green point referring to in the image?  
=====

Options  
A. The green point refers to a towel.  
B. The green point refers to a toilet.  
C. The green point refers to a sink.  
D. The green point refers to a bathtub.  
=====

Answer: B

✓
DeepSeek-VL2: B

**Point – Reference**

Question: What is the red point referring to in the image?  
=====

Options  
A. The red point refers to a cone.  
B. The red point refers to a ball.  
C. The red point refers to a flag.  
D. The red point refers to a person.  
=====

Answer: D

✗
DeepSeek-VL2: B

Figure 12: Qualitative results of point shape in Stage 1 evaluation.

**Emotion Recognition**

Question: What emotion is the person showing in the area highlighted by red bounding box?

Options

- A. The detected facial expression is disgusted.
- B. The detected facial expression is happiness.
- C. The detected facial expression is fearful.
- D. The detected facial expression is sleepy.

Answer: B

✓
Qwen2.5-VL-72B: B

**Emotion Recognition**

Question: What emotion is the person showing in the area highlighted by red bounding box?

Options

- A. The detected facial expression is flirty.
- B. The detected facial expression is surprised.
- C. The detected facial expression is sleepy.
- D. The detected facial expression is neutral.

Answer: D

✗
Qwen2.5-VL-72B: B

**Street View Recognition**

Question: What does the red bounding box highlight in this street scene?

Options

- A. This is a pedestrian crossing sign for safety.
- B. This is the backside of a sign with no primary information.
- C. This is a directional arrow on the road surface.
- D. This is a traffic light indicating a stop signal.

Answer: B

✓
InternVL2.5-78B: B

**Scribble – Existence**

Question: What does the red bounding box highlight in this street scene?

Options

- A. This is a traffic island directing vehicle flow.
- B. This is a designated parking zone for vehicles.
- C. This is a pedestrian crossing area with a raised platform.
- D. This is a landscaped median strip for aesthetic purposes.

Answer: A

✗
InternVL2.5-78B: C

Figure 13: Qualitative results of facial emotion recognition task and street view recognition task.

**Medical Image Analysis**

Question: Please assess the pathological characteristics of this region.

Options

- A. The highlighted area represents benign hyperplasia of the bladder urothelium, characterized by increased cell proliferation without malignant transformation.
- B. The highlighted area suggests bladder urothelial carcinoma, a malignancy arising from the urinary bladder's epithelium.
- C. The highlighted area indicates bladder squamous cell carcinoma, a cancer developing from squamous cells lining the bladder.
- D. The highlighted area suggests bladder adenocarcinoma, a malignancy originating from glandular cells within the bladder.

Answer: B

✓
Qwen2.5-VL-72B: B

**Medical Image Analysis**

Question: Please assess the pathological characteristics of this region.

Options

- A. The highlighted section demonstrates characteristics of liver metastasis from colorectal adenocarcinoma, indicating spread from the colon or rectum.
- B. This area exhibits signs of cholangiocarcinoma, a cancer arising from the bile ducts within the liver.
- C. The annotated region displays characteristics of lung squamous cell carcinoma, which arises from the squamous cells lining the airways.
- D. The annotated region shows features of hepatocellular carcinoma, a type of liver cancer originating from the liver's main functional cells.

Answer: C

✗
Qwen2.5-VL-72B: A

**3D Object Recognition**

Question: Given a top-down and a front view (from south to north) of a room, identify the object marked by the red digit tag and specify its position.

Options

- A. This is a fridge, located at the north-east of the room.
- B. This is a cabinet, located at the north-east of the room.
- C. This is a fridge, located at the south-west of the room.
- D. This is a microwave, located at the north-east of the room.

Answer: A

✓
DeepSeek-VL2: A

**3D Object Recognition**

Question: Given a top-down and a front view (from south to north) of a room, identify the object marked by the red bounding box and specify its position.

Options

- A. This is a dining table, located at the center of the room.
- B. This is a dining table, located at the north-east of the room.
- C. This is a side table, located at the north-east of the room.
- D. This is a coffee table, located at the north-east of the room.

Answer: B

✗
DeepSeek-VL2: D

Figure 14: Qualitative results of medical image analysis task and 3D object recognition task.

**GUI Element Recognition**

Question: Can you recognize the graphical user interface (GUI) element highlighted by the red digit tag?

Options

A. The UI control highlight by red digit tag corresponds to the "display a tide chart for coastal areas" functionality.  
 B. The UI control highlight by red digit tag corresponds to the "open mind2web folder" functionality.  
 C. The UI control highlight by red digit tag corresponds to the "show a summary of extreme weather alerts" functionality.  
 D. The UI control highlight by red digit tag corresponds to the "show a summary of daylight hours" functionality.

Answer: B

 Qwen2.5-VL-72B: B

**GUI Element Recognition**

Question: Can you recognize the graphical user interface (GUI) element highlighted by the red digit tag?

Options

A. The UI control highlight by red digit tag corresponds to the "view a list of nearby weather stations" functionality.  
 B. The UI control highlight by red digit tag corresponds to the "check weather on tuesday" functionality.  
 C. The UI control highlight by red digit tag corresponds to the "display hourly weather forecast" functionality.  
 D. The UI control highlight by red digit tag corresponds to the "show a summary of marine weather conditions" functionality.

Answer: C

 Qwen2.5-VL-72B: C

**Visual Relation Prediction**

Question: What is the object that is in front of the thing highlighted by the red digit tag?

Options

A. The object is the traffic light.  
 B. The object is the fence.  
 C. The object is the house.  
 D. The object is the toilet.

Answer: B

 DeepSeek-VL2: B

**Visual Relation Prediction**

Question: What is the object that is on the thing highlighted by the red bounding box?

Options

A. The object is the food.  
 B. The object is the remote.  
 C. The object is the cat.  
 D. The object is the toaster.

Answer: B

 DeepSeek-VL2: A

Figure 15: Qualitative results of GUI element recognition task and visual relation prediction object recognition task.